2016-06-01

# Friction Bit Joining of Dissimilar Combinations of GADP 1180 Steel and AA 7085 – T76 Aluminum

Lorne Steele Atwood
*Brigham Young University*

# Friction Bit Joining of Dissimilar Combinations of GADP 1180 Steel and AA 7085 – T76 Aluminum

Lorne Steele Atwood

A thesis submitted to the faculty of
Brigham Young University
in partial fulfillment of the requirements for the degree of

Master of Science

Michael P. Miles, Chair
Charles R. Harrell
Jason M. Weaver

School of Technology

Brigham Young University

June 2016

ABSTRACT

Friction Bit Joining of Dissimilar Combinations of
GADP 1180 Steel and AA 7085 – T76 Aluminum

Lorne Steele Atwood
School of Technology, BYU
Master of Science

Friction Bit Joining (FBJ) is a method used to join lightweight metals to advanced high-strength steels (AHSS). The automotive industry is experiencing pressure to improve fuel efficiency in their vehicles. The use of AHSS and aluminum will reduce vehicle weight which will assist in reducing fuel consumption.

Previous research achieved joint strengths well above that which was required in three out of the four standard joint strength tests using DP980 AHSS and 7075 aluminum. The joints were mechanically tested and passed the lap-shear tension, cross-tension, and fatigue cycling tests. The t-peel test configuration never passed the minimum requirements.

The purpose of continuing research was to increase the joint strength using FBJ to join the aluminum and AHSS the automotive industry desires to use specifically in the t-peel test. In this study FBJ was used to join 7085 aluminum and GADP1180 AHSS. The galvanic coating on the AHSS and its increased strength with the different aluminum alloy required that all the tests be re-evaluated and proven to pass the standard tests.

FBJ is a two-step process that uses a consumable bit. In the first step the welding machine spins the bit to cut through the aluminum, and the second step applies pressure to the bit as it comes in contact with the AHSS to create a friction weld.

Keywords: Lorne Atwood, friction bit joining, FBJ, dissimilar metals, advanced high-strength steel, aluminum, GADP1180. Automotive manufacturing, joint strength, welding machine.

# ACKNOWLEDGEMENTS

I am thankful to Honda and the Department of Energy for providing the funding for this research. I am also thankful to Oakridge National Labs for the collaborative efforts made in this research.

I would like to express sincere appreciation to the many people who have contributed to the improvement of the friction bit joint. I have been able to work with a great team here at BYU: Shane Wood, Derek Thompson, Brad Burgess, and Kevin Shirley. They have helped substantially in improving the friction bit process and it has been enjoyable to work with them. I would like to thank Dr. Mike Miles for his support and guidance as my committee chair and as a mentor and friend. Thank you also to the other committee members and professors in the manufacturing program at Brigham Young University.

Most importantly I would like to thank my wife and best friend, Annette, for the love, support and motivation she has provided during this time.

TABLE OF CONTENTS

LIST OF TABLES

LIST OF FIGURES

# 1 INTRODUCTION

As government regulations on fuel requirements become more restrictive, the desire for lighter weight vehicles increase. In the past, the vehicle frame was made of steel; but now light metals, like aluminum, are being introduced into the body structure(Lim, Squires et al. 2015). Steel and aluminum can be joined by self-piercing riveting, as long as the steel is ductile. However, the newer advanced high strength steels (AHSS) being used for automotive structures are too hard to use self-piercing rivets. Friction Bit Joining (FBJ) is one solution to this problem. In FBJ, a consumable bit is driven into the two materials. The softer metal (Aluminum) is placed on top, and the bit cuts through this top layer, then friction welds to the harder metal (GADP1180) underneath. The head of the bit holds the aluminum to the steel, where the primary bond is between the steel sheet and the steel bit. The joining bit is consumable, meaning that it is left in the workpiece at the end of the process and forms an integral part of the weld(Miles, Hong et al. 2013). The strength of the resulting joint has been shown to be more than the strength of the aluminum in lap-shear test. The use of FBJ helps prevent brittle microstructure from developing in the weld(Huang, Sato et al. 2009).

The ability to join aluminum to steel has many applications. Reducing the weight of vehicles, whether that is for land, sea, or air will also reduce the consumption of the fuel required to power them. Combining dissimilar metals also allows us to exploit the strengths of each material, whether that is the strength, ductility, corrosion resistance or any other property, while

minimizing their weaknesses. One unique thing about FBJ is its ability to combine a rivet-like bond and a weld bond. This combination can remove the difficulties encountered that are associated with metallurgical incompatibility(Sun and Karppi 1996).

## 1.1 Standard Tests

There are four standard tests for measuring the strength of the welds: lap-shear, cross-tension, t-peel, and fatigue. These tests are based on AWS, specifications for automotive weld quality. Since these standards are for like metals not dissimilar metals we are using numbers supplied by our automotive sponsor (Table 1). A piece of AHSS (1.2mm thick) and aluminum (2mm thick) each measuring 125mm x 40mm are used as sample coupons for all but the cross-tension test. The cross-tension test uses coupons 150mm x 50mm with holes positioned close to the ends as shown in Figure 1-2. It is imperative to have the softer metal, the aluminum, positioned so that the bit can cut through it before it welds to the AHSS. The weld should be centered in the area where the aluminum and steel overlap.

**Table 1 Sponsor Joint Strength Standards**

| Test | Steel-Al Mechanical Joint |
|---|---|
| T-Peel | >1.5kN |
| Cross-Tension (CTS) | >1.5kN |
| Lap-Shear Tension (TSS) | >5kN |
| TSS Fatigue ($10^7$) | 0.10 - 0.75kN |

### 1.1.1 Lap-Shear Test

The lap-shear test (Figure 1-1) consists of positioning one coupon of each metal in a straight line overlapping the ends of the coupons by 20mm and applying an FBJ to the coupons. The strength test is performed by gripping the other ends of the coupons in a tension testing machine and pulling the coupons apart while measuring the maximum load before the bond is broken. The minimum load requirement for the bond to pass this test is 5kN.


**Figure 1-1 Lap-Shear Test Layout**

### 1.1.2 Cross-Tension Test

The cross-tension test (Figure 1-2) consists of overlapping the coupons perpendicular to one another creating a cross. As mentioned previously these coupons are larger than the standard coupons used in the other tests. Both ends of each coupon are gripped with the top coupon being pulled up while the bottom coupon is pulled down in a tension testing machine while measuring the maximum load before the bond is broken. The minimum load requirement for the bond to pass this test is 1.5kN.

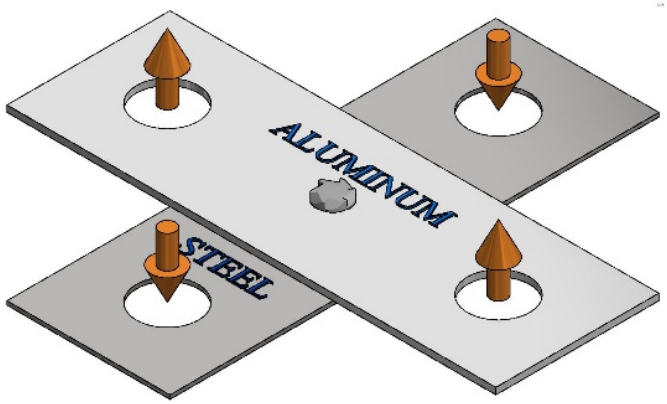


**Figure 1-2 Cross-Tension Test Layout**

### 1.1.3 T-Peel Test

To conduct the t-peel test a $90^0$ bend is made 40mm from one end of the standard coupon creating an L shape in both the aluminum and AHSS coupons. The L shaped coupons are placed in opposite directions with the shorter, bent ends of the L shapes joined together with an FBJ. The long ends of the L shape are gripped in a tension testing machine and pulled apart (Figure 1-3). The maximum load before the bond breaks is required to exceed 1.5kN for the weld to pass this test.

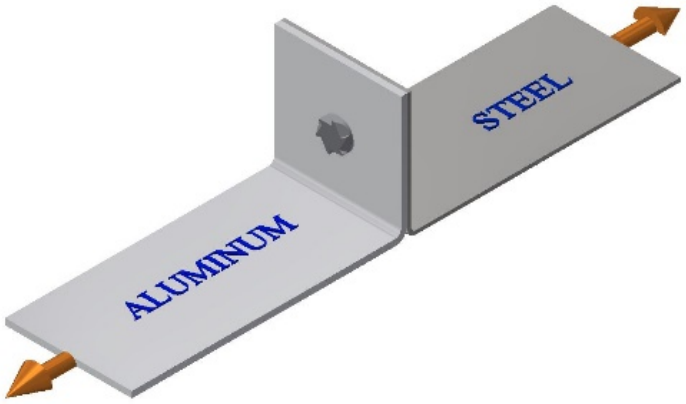


**Figure 1-3 Peel Test Layout**

### 1.1.4 Fatigue Test

The fatigue test is setup the same way as the lap-shear test (Figure 1-1) but when the coupons are placed in the tension testing machine the loads are cycled between 0.1kN and 0.75kN at 20Hz. The test must run for over ten million cycles for the bond to pass. Then the sample should still be able to pass the lap-shear test.

## 1.2 Previous Research

Previous research testing achieved sufficient strength in three out of the four required tests, using DP980 and AA7075 coupons and a machined bit made of 4140 steel alloy. The FBJ with these materials did not pass the t-peel test. However, the automotive industry partner is now requiring the use of new materials, AA 7085 and GADP1180; therefore the results may be different for this research. The former bit material (4140) is not easily cold formed. The cold forming process is less expensive to manufacturing large quantities of the bits than machining them. A new bit material that can be both cold formed and friction welded to the GADP1180 with sufficient strength to achieve required results for all four tests needs to be found.

## 1.3 Purpose of the Research

There is an increasing demand for the automakers to improve fuel economy, crash safety, and vehicle performance. Combining high strength aluminum and AHSS to reduce the weight of the vehicle(Chen and Kovacevic 2004), while increasing the strength of the vehicle, is one of the options that the automotive industry is pursuing to improve fuel efficiency, crash safety, and vehicle performance. The steel industry has responded with creating higher strength steels in the AHSS. The properties of these steels include reasonable formability, ductility, and high strength. The use of AHSS allows automakers to use thinner sheet steels in the body structure while

having high energy absorption for the dynamic loading required for crash worthiness(Kuziak, Kawalla et al. 2008).

The purpose of this research is to improve the FBJ welding process to achieve sufficient results in all four of the standard tests with the new AHSS and aluminum materials and with a new bit material that can be cold formed. This will allow the automotive industry to implement FBJ technology in joining dissimilar metals which can improve the many aspects of their vehicles.

## 1.4 Research Hypotheses

In order to meet the demands of this research there are three hypotheses to be tested.

1. FBJ can create a spot joint between galvanized DP 1180 steel and AA 7085-T76, where the strength exceeds minimum standards in lap-shear, cross-tension, fatigue, and t-peel configurations.
2. A low carbon steel alloy, like 1018, can be used for the bit material in order to create joints of acceptable strength between galvanized DP 1180 and AA 7085-T76.
3. A FBJ with this material combination can achieve the desired nugget pull out failure mode 100% of the time.

All prior work in FBJ development has been done using combinations of bare DP 980 steel and AA 5754, AA 5182, and AA 7075 aluminum. A higher strength alloy like DP 1180 may cause difficulties in welding, especially if the material is galvanized. The aluminum alloy is less of a concern, because we are not technically welding it; we are cutting through it with the joining bit and compressing it to the steel sheet underneath. Also, prior joining bits have been made from alloy steels like 4140. However, these steels are expensive, so the current research will

investigate the bonding properties that can be achieved with cheaper, plain carbon steels like 1018.

## 1.5 Objectives

The objectives of this research are to improve the welding process by adjusting the spindle speed, plunge rate, plunge depth and dwell times, as well as change the bit design and material. Some bit design changes will be varying the cutting surface and size to improve joint strength for the t-peel test while maintaining the automotive standards in the other tests.

## 1.6 Methodology

The welding process currently has 2 steps. The first is to cut through the AA7085, the second is to apply pressure and spindle speed to the bit to create a friction weld between the bit and the GADP 1180. Our experiments will be conducted on a C frame welding machine designed specifically for FBJ (Figure 3-1). The experiments will be conducted to determine the optimum parameter values for the process. The variables that will be involved for the welding machine are: spindle speeds, depth of plunge, rate of plunge and dwell times. The bit material will also be a variable. For example, we plan to try steel alloys such as 4130, and plain carbon steels such as 1018 which are both better for cold forming. Once the welds are made, they will be tested to determine strength for the different welding parameters. The three configurations that will be tested are lap-shear tension, cross-tension, and t-peel. We will also perform a fatigue life study using lap-shear tension specimens. For each test we will use 15 specimens in order to generate statistically meaningful data for each of the three primary tests (lap-shear, cross-tension, and t-peel).

### 1.6.1 Materials

The dissimilar metals that are joined for the purposes of this research are aluminum and steel. Specifically, these materials are 2 mm thick AA 7085-T76 aluminum which is frequently used in aerospace application(Ram 2015), and 1.2 mm thick galvanized AHSS (GADP 1180). GADP1180 is particularly suited for use in the automotive industry due to its mechanical strength, high work hardening rate, and high uniform and total elongation(Bhagavathi, Chaudhari et al. 2011). The galvinized coating helps reduce corrosion and is an intergal part of this research.

Materials experimented with for bit manufacture are half-hard AISI 4140 and 4130 alloy steel, O1 tool steel, and 1018 low carbon steel. The cutting surface of the bits are produced using an Okuma CNC lathe (Figure 1-4) to machine all but the head. The head is cold formed with a die press (Figure 1-5).


**Figure 1-4 Okuma Lathe**

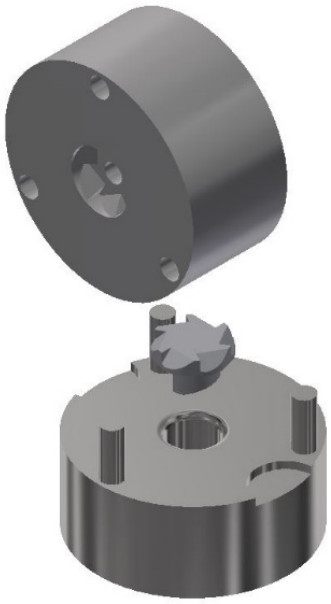

**Figure 1-5 Manual Die Press to Form Head**

The 1018 steel is among the most commonly available grades in the world. The use of 1018 for this application provides access to a material that is easily formed, machined, welded and fabricated. Its higher Mn content allows it to be hardened to the 42 RC range which makes it hard enough to create a bond with the galvanized DP 1180. As the automotive industry implements the use of FBJ it will require millions of friction bits. The ability to produce these efficiently and inexpensively will make the use of 1018 favorable as the material of choice.

### 1.6.2 Experiments

Coupons of each material were used in the experiments. For the lap-shear, fatigue, and t-peel tests the coupons were 40 mm wide by 125 mm long with the metal grain running in the long direction. For the cross-tension tests the coupons were 50 mm wide by 150 mm long with two 19 mm holes spaced 100 mm apart and centered in the coupon.

Joint strength in t-peel was tracked and independent variables were manipulated based on the results of the mechanical testing. Mechanical testing is a simple and fast method to evaluate the strength of the joint. Mechanical testing was also used to confirm that the changes made to the FBJ did not adversely affect the cross-tension, lap-shear, and fatigue tests.

Microstructure of the joint was compared with the joint strength and standard failure modes. Figure 1-7 shows the edges of the heat affected zone (HAZ), the aluminum and bit steel flow, and the surface between the bit and the GADP 1180. Comparing the microstructure of the different bit designs guided us in making design changes to the bit and the weld parameters.

### 1.6.3 Microscope

The internal features of the weld are viewed by sectioning a welded sample (Figure 3-18) through the middle of the weld and then mounting the sectioned sample in a puck and polishing it. The resultant puck is viewed using a microscope see Figure 1-6 and Figure 1-7.

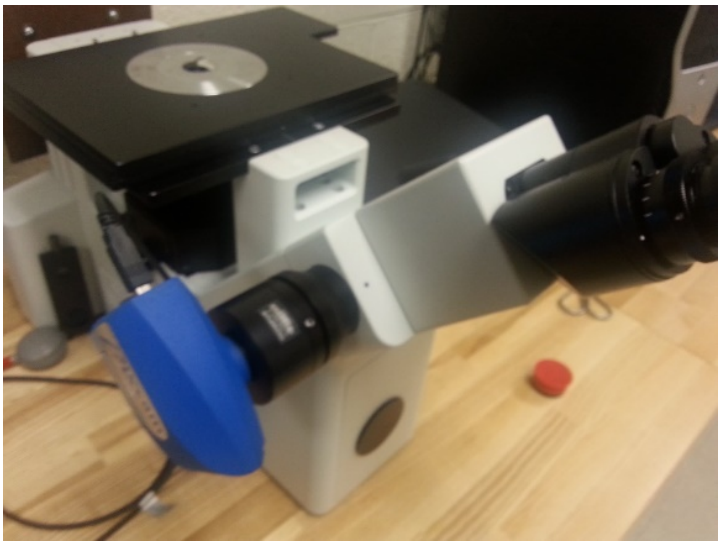

**Figure 1-6 Microscope**

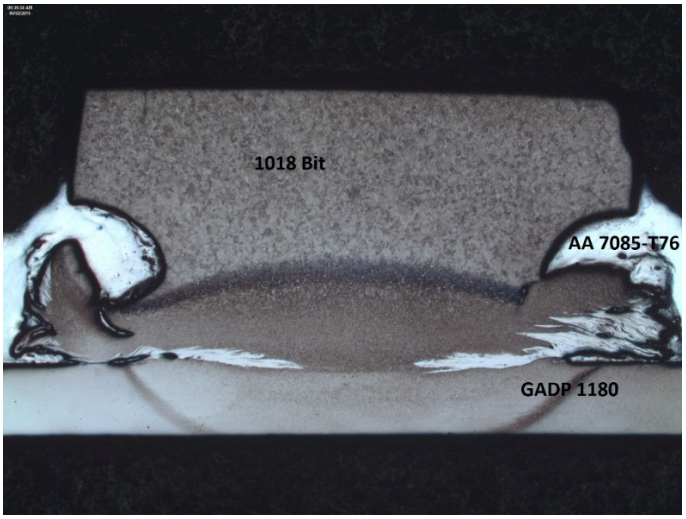


**Figure 1-7 Macro-Section View**

### 1.6.4 Independent Variables

- Welding machine spindle speed, plunge rate, and dwell time.
- Bit cutting surface, diameter and profile.
- Bit material, composition and hardness.

## 1.7 Delimitations and Assumptions

This research only investigates the joining of AA 7085-T76 aluminum and AHSS GADP1180. The focus was on creating a weld that was able to pass the t-peel test. Conclusions may be drawn for joining other materials and applications.

## 1.8 Definitions of Terms

AHSS – advanced high-strength steel (steel that yields at 560 MPa or above)

DP – Dual phase steel that has a ferrite and martensitic microstructure

EDM – electronic discharge machining. Two types were used during this work: wire and plunge.

FBJ – friction bit joining. A technology that uses a consumable bit to spot join metals.

GA – galvanic coating applied to steel.

GADP 1180 – galvanized dual phase high strength steel with an ultimate tensile strength of 1180 MPa

HAZ – heat-affected zone is the area within a material that has changed properties due to welding or some other heat intensive process.

RSW – resistance spot welding is a fusion-welding process that uses electrodes to clamp the sheet metals together and pass a current through them which produces the necessary welding heat.

RPM – revolutions per minute

SPR – self-piercing riveting is a cold forming process that uses a die set to force a rivet into sheet metal without predrilling a hole.

UTS – ultimate tensile strength.

# 2 LITERATURE REVIEW

## 2.1 Introduction

Lightweight construction is considered one of the most important future technologies. It has impacted the automotive industry through the development of new materials, products, technologies and environmental affects (Albrecht, Baumann et al. 2013). In recent years there has been an increased emphasis on the development of new AHSS, particularly for automotive applications(Matlock and Speer 2009).

Articles in the literature review discuss the current methods used to join dissimilar material, specifically AHSS and aluminum. The advantages and limitation of these methods are examined and compared with how FBJ can fill the gaps. These articles present some challenges in joining dissimilar metals like the varying melting temperatures, ductilities, and hardness. The differences in fusion temperature makes it especially challenging when joining AHSS and aluminum(Torkamany, Tahamtan et al. 2010). AHSS has higher contents of alloying elements than lower strength steels. There are a variety of technologies that attempt to overcome these challenges.

## 2.2 Traditional Methods for Dissimilar Material Joining

Friction stir welding (FSW) was developed in 1991(Nandan, DebRoy et al. 2008). The advantages of FSW are a minimum heat affected zone (HAZ), short cycle times, and good

quality welds. Temperatures that are developed through friction are found to be about 80% of the melting point of the workpiece metal. Friction stir spot welding (FSSW) is the most commonly used method for joining aluminum and steel sheet metal in the automotive industry. However, its applications are limited, because friction stir spot welds of aluminum and steel have been shown to have relatively low joint strength. "In the aluminium/steel system, intermetallic compounds are a major problem, in general the formation of intermetallic phases being considered undesirable" (Yilbaş, Şahin et al. 1995). For welding steel, FSSW can reduce the thermal effect to the welded material, because it is a solid-state process. However, the high-speed, high-volume, and cost-conscious nature of the automotive industry restricts the implementation of FSSW, because tooling costs are quite high compared to resistance spot welding (RSW).

To assist RSW in creating a solid joint between dissimilar metals, a coated process tape is placed between the electrodes and the metal. The properties of the coated tape varying depending on which metal the electrode is near in order to achieve the targeted heat for the weld (Gendo, Nishiguchi et al. 2007). RSW has been proven to join AHSS to softer metals, but the presence of micro cracks in the joint and the tightly controlled operational conditions make RSW limited in production (Miles, Karki et al. 2014).

Two other methods for joining: clinching and self-piercing rivets (SPR) have limited effectiveness in joining high strength dissimilar metals. Clinching is a cold forming process that forms one piece of metal into another piece using a die to create a mechanical lock between the two metals (Hamel, Roelandt et al. 2000). SPR drives the shank of the rivet though the upper sheet metal and flares the skirt of the rivet in the lower sheet. This creates an interlock. SPR is a cold forming process that uses a rivet that is forced through the sheet metal into a die to form a mechanical lock between the metals. It is also a relatively fast process and is low energy(Abe,

Kato et al. 2009). A limitation of this process is that piercing the rivet into the AHSS is difficult, because the strength of the steel sheets approach that of the rivet. Increasing the strength of the rivet is also limited(Mori, Kato et al. 2006). The size of the riveting gun also restricts access to certain joint areas. Due to the crevices and surface irregularities, corrosion is also a concern(Barnes and Pashby 2000). Both of these methods require ductile deformation of both the metals(Miles, Feng et al. 2010).

Spot friction welding (SFW), is a non-traditional welding method that uses a process similar to linear friction stir welding (FSW). Rather than move the tool in a transverse direction it is instead retracted from the weld when the stirring is complete. This process has been successful for joining similar metals like aluminum to aluminum (Pan, Joaquin et al. 2004). There has been success using the SFW process joining aluminum to steel and the process produces welds with lap-shear strength of around 2KN (Gendo, Nishiguchi et al. 2007).

Adhesives are another common technique for joining dissimilar metals. A few advantages of adhesives are: they do not distort the components being joined; a continuous bond is produced rather than a localized point contact; the equipment is lower in cost; and the bonds are inherently high strength in shear. A few disadvantages are: adhesives are generally an epoxy or solvent-based compound creating environmental concerns; many structural adhesives require heat curing; and the joints created are weak in t-peel. This t-peel limitation is especially worrisome for crashworthiness in vehicles(Barnes and Pashby 2000).

## 2.3 FBJ Welding

Traditional methods meet some of the needs for joining AHSS and aluminum. There are still gaps in their performance and processes. Friction bit joining (FBJ) overcomes many of these

limitations while still meeting performance and manufacturing requirements. FBJ is being tested for joining dissimilar metals and is achieving joint strength higher than the other joining methods (Miles, Hong et al. 2013). FBJ is a relatively new technology. It has been proven to have comparable joint strength to other methods of joining while having more flexibility with the materials being joined.

Research on FBJ includes areas such as feasibility, optimal parameters, and bit alloy and design (Miles, Kohkonen et al. 2009). For example, a 'fluted' bit has been compared to a 'flat' bit design. The flutes were intended to aid in removing chips that form during the cutting phase of joining. The 'fluted' design was found to produce more consistent results. The research has shown that weld cycle time produces improved joint strength. Research has also shown that the material and design of the bit will affect joint strength. Defect-free joints have been successfully produced by FBJ. There are 4 methods to test the joint strength and previous research has been able to achieve sufficient strength in 3 of the 4 tests, lap-shear, cross-tension, and tension fatigue using the AHSS and aluminum. The t-peel test has not achieved sufficient strength with any of the materials. The other tests have exceeded the testing requirements using different materials than this study is using, DP980 and AA 7075-T6 instead of GADP1180 and AA7085-T76, the results for those test will have to be confirmed in this research with the new materials.

# 3 METHODOLOGY/EXPERIMENTAL DESIGN

## 3.1 Summary

The hypotheses of this research were explored using welds made through friction bit joining (FBJ). The weld strengths of various bit designs were compared and the effects of varying the weld parameters on the weld strengths were evaluated. Bit design variations consisted in enlarging the cutting surface diameter of the bit and changing the steel alloy the bit was made of. There are many possible combinations in the welding process, with the machine capable of up to four different stages, with four adjustable variables in each stage.

## 3.2 FBJ Machine

The machine used for FBJ experimentation (Figure 3-1) was made by MegaStir Technologies and was designed, engineered and built for testing FBJ (Squires 2014). The main servo motor allows the spindle speed, measured in revolutions per minute (RPM), to be varied up to a maximum of 4000 RPM. There is also a servo motor mounted to the frame to control the speed of the Z movement which is able to apply high loads to the bit during the welding cycle. There is a brake device on the spindle to facilitate the rapid stopping required for the welding process. Below the spindle there is a fixture (anvil) to position and secure the welding specimens (coupons) during the welding process. The anvil also has a load cell built in it directly below the spindle to measure loads during the welding cycle. This load cell also assists in securing the

coupons by measuring the force the clamping system places on the coupons while securing them in place. A locating jig is attached to the anvil to align the coupons prior to welding. There is software to operate the machine as an interface for controlling the different parameters of the weld. Parameters like spindle speed (RPM), Z axis velocity (inches per minute), Z travel (inches) and dwell time (milliseconds) can be set for each of four stages. If all four software stages are not required some can be deactivated. Two stages typically work well for the FBJ application. Stage one is cutting through the aluminum, stage two is welding to the AHSS. The software also gathers information from sensors on the machine that provide feedback and information about the spindle speed, spindle torque, Z force, Z motor torque, Z axis velocity, weld duration, and tool depth. Figure 3-1 shows a picture of the FBJ machine.

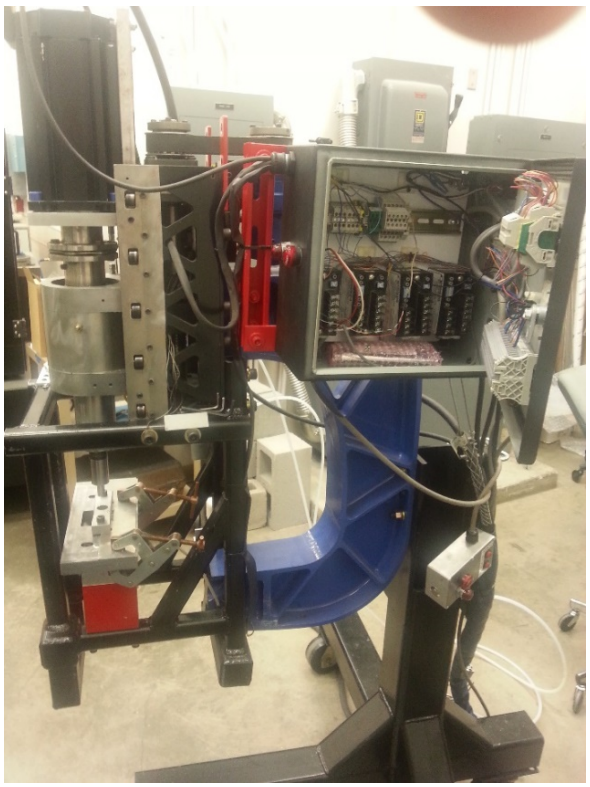

**Figure 3-1 FBJ Machine**

## 3.3 FBJ Process

FBJ is a two-step process using a consumable bit. When creating a joint between an aluminum sheet and a steel sheet, where the aluminum is on top, the first step is to drill through the aluminum with a rotating bit. The second step is to create a weld with the steel by frictional heating of the rotating bit. Figure 3-2 shows a schematic of the FBJ joint.

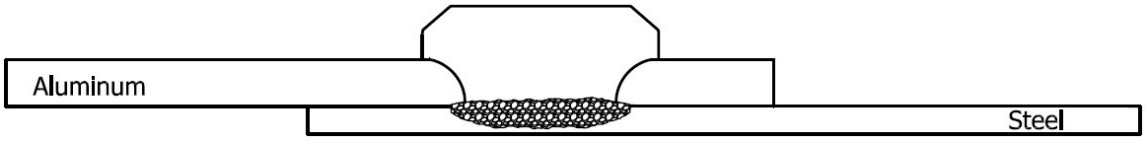


**Figure 3-2 FBJ Process Schematic**

During the course of experimenting with different process parameters, we found that it can be beneficial to impose a dwell during the cutting stage at the moment that the bit touches the steel coupon surface. The dwell allows the spindle to continue rotating at high speed, without continuing to plunge. This creates some additional heating before the plunge resumes and the bonding begins, as the bit is compressed against the steel and the spindle continues to rotate at high speed. The steel coupon is too hard to cut with the consumable bit therefore a weld can be created by frictional heating. At the end of the last stage the spindle stops and pressure is maintained for a moment to allow some cooling, before the driver is returned to its top position.

## 3.4 Bit Properties

The general bit design has been the topic of research in previous master's theses. The material selection and cutting diameter have been modified from that research. The materials that were tested in this research were 4140, O1, 4130 and 1018 allow steels. The cutting

diameter has been enlarged in .38 mm (0.015 inch) increments and a “nub” was added to improve the penetration of the weld into the GADP 1180. Figure 3-3 shows the final bit design.

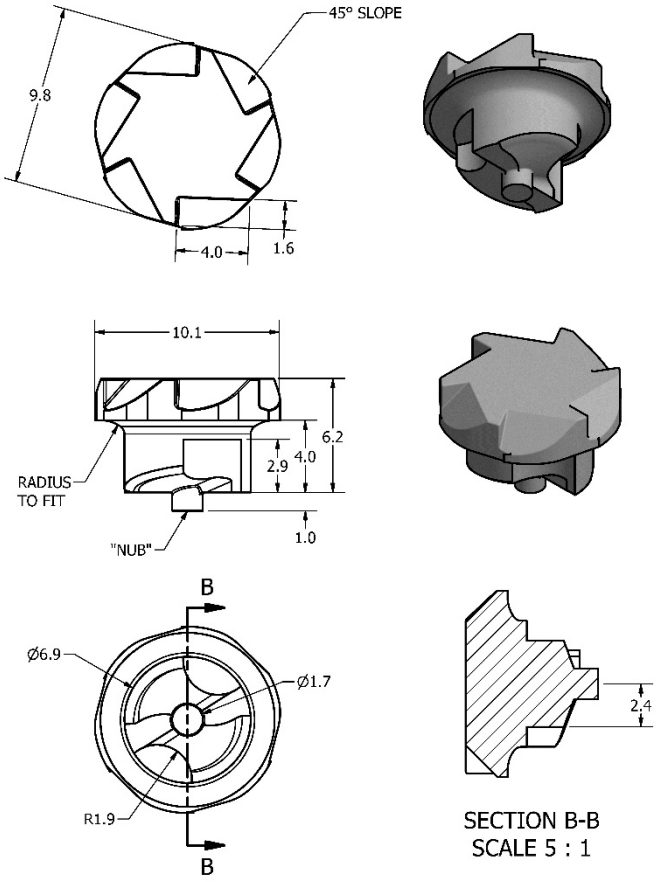


**Figure 3-3 Bit Design**

## 3.5 Specification for the Coupons

Coupons were cut on a hydraulic shear out of aluminum and steel to 125 mm long x 40 mm wide. This coupon size was changed from the previous research which had a coupon size of 100 mm x 25 mm. The grain direction is in the long direction. The steel and the Aluminum are 1.2 and 2 millimeters thick respectively.

The steel used has varied throughout the term of the experiments. The first steel used was DP980. DP980 was used for the previous research also. The material requirement changed to DP1180 and then GADP1180. So the final conclusions will be based on this steel.

## 3.6 Required Standards for Joint Strength

The standard joint strengths, as determined by a sponsor, Honda, are given in Table 2. For this research the "Steel-Al Mechanical Joint" is the required strengths used, the steel baseline is given only as a reference.

**Table 2 Automotive Joint Strength Standards**

| Joint strength standards | | |
|---|---|---|
| Test | Steel Baseline | Steel-Al Mechanical Joint |
| T-Peel | >2kN | >1.5kN |
| Cross-Tension (CTS) | >5kN | >1.5kN |
| Lap-Shear Tension (TSS) | >18kN | >5kN |
| TSS Fatigue ($10^7$) | 0.10 - 0.75kN | 0.10 - 0.75kN |

## 3.7 Testing Procedures

### 3.7.1 Welding Parameters

The tests are run with three to five specimens tested every time a weld parameter is modified. Having multiple specimens increases the probability that the average results are an accurate assessment of the weld performance. The parameters are evaluated on an Instron tension testing machine using mechanical testing for the welded specimens and comparing the peak loads the

joints were able to attain before failure. The parameters included the spindle speed, plunge rate, plunge depth and dwell time for up to 4 stages. The settings from previous research were;

- Stage 1 (cutting) – spindle speed 2000RPM, plunge rate 1.25 inches per minute (IPM), plunge depth -0.080 inches.
- Stage 2 (welding) – spindle speed 2500 RPM, plunge rate 1.25 IPM, plunge depth of -0.187 inches.
- Stages 3 and 4 were not used.

For this research we varied the parameters. The "nub" on the new bit required that we plunge deeper at each stage to compensate for the extra distance the "nub" created. We adjusted the parameters with the final settings being;

- Stage 1 (cutting) – spindle speed 4000 RPM, plunge rate 28 IPM, plunge depth -0.127 inches, Dwell 50 milliseconds.
- Stage 2 (welding) – spindle speed 4000 RPM, plunge rate 4.5 IPM, plunge depth -0.225 inches.
- Stages 3 and 4 were not used.

### 3.7.2 T-Peel Test

The t-peel test was the main test configuration examined in this research. The coupons used were 125 mm x 40 mm before they were bent. In previous research the coupons were 100mm x 25mm before bending. The t-peel test is used for evaluating the crash worthiness of joints. For the t-peel test the anvil portion of the machine had to be re-designed to allow for the coupons to

be bent before they were welded (Figure 3-4). In previous research the coupons were welded flat and then bent for the t-peel test. Bending the coupons after they were welded may have been adding strain to the weld before testing on the Instron machine (Figure 3-10). We redesigned the anvil so we could pre-bend the coupons to remove the chance of damaging the weld before testing.

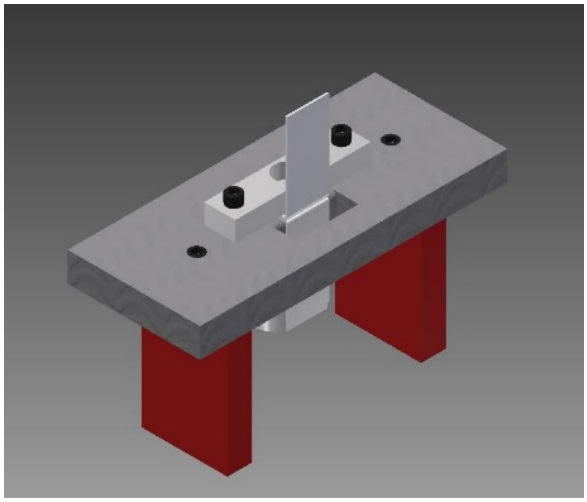

**Figure 3-4 Anvil Design**

The specifications given from Honda suggest a 5mm internal radius for the bend. The steel coupon is able to bend this tight while at room temperature without breaking (Figure 3-5 and Figure 3-6).

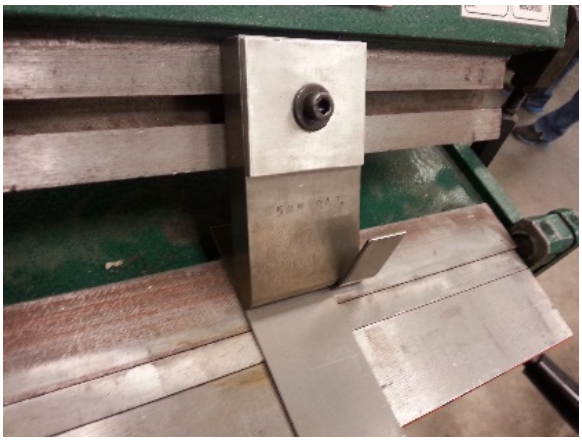

**Figure 3-5 Steel Coupon Set for Bending**

**Figure 3-6 Steel Coupon Bent**

The 7085-T76 aluminum is too brittle to make the 5mm radius bend without breaking or cracking while at room temperature. We Pre-heated the oven to $40^0$C and placed twenty to thirty (20-30) coupons in the oven and let them soak for thirty minutes (Figure 3-7). We removed the coupons from the oven and kept them in an insulated bag until they were placed on the brake for

bending. The bending process was the same as used for the steel coupons (Figure 3-5 and Figure 3-6) except that the aluminum was kept warm until the procedure. No cracking or breaking occurred following this procedure.

**Figure 3-7 Oven for Warming Aluminum Coupon Before Bending**

The new anvil allows the bent coupons to be aligned and clamped so that the bit will be 20 mm from each of the 3 edges (Figure 3-8). When the coupons are welded they form a 180 degree total plane as shown in Figure 3-9 creating the t-peel test specimens. The specimens were then tested on the Instron machine (Figure 3-10) pulling apart at 10.16 mm/min.

**Figure 3-8 Welding of Bent Samples**

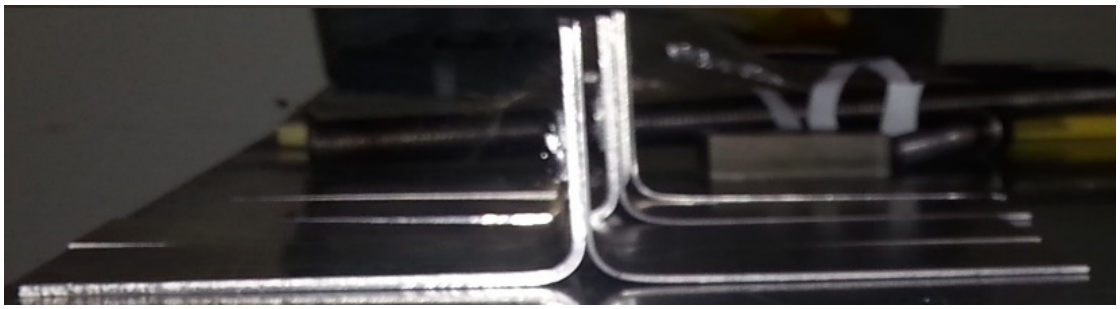

**Figure 3-9 Welded T-Peel Test Coupons**

**Figure 3-10 T-Peel Test as the Weld is Failing.**

The Instron software records the extension and load on the specimen at the time of failure, the peak load obtained before failing; and a summary of the results including max, min, standard deviation, and mean (Table 3).

**Table 3 Instron Tensile Test Output for a Set of 5 T-Peel Test Specimens**

| | Load at Machine Break (N) | Extension at Machine Break (mm) | Extension at Machine Peak Load (mm) | Load at Machine Peak Load (N) |
|---|---|---|---|---|
| 1 | 1178.77883 | 38.73500 | 30.17520 | 1918.96297 |
| 2 | ----- | ----- | 26.28900 | 1870.03253 |
| 3 | 1626.26996 | 10.92200 | 10.41400 | 1711.23100 |
| 4 | 652.10935 | 3.81000 | 3.83540 | 652.10935 |
| 5 | 1290.87402 | 49.98720 | 30.40380 | 2009.70670 |
| Maximum | 1626.26996 | 49.98720 | 30.40380 | 2009.70670 |
| Minimum | 0.00000 | 0.00000 | 3.83540 | 652.10935 |
| Standard Deviation | 635.82898 | 22.31800 | 12.29086 | 558.59914 |
| Mean | 949.60643 | 20.69084 | 20.22348 | 1632.40851 |

### 3.7.3 Lap-Shear Tension

The same coupon sizes that were used for Lap-Shear were the same as those used for the t-peel test, without being bent. A coupon of each material is placed in a positioning jig (Figure 3-12) on the FBJ machine with a 20 mm overlap (Figure 3-11).

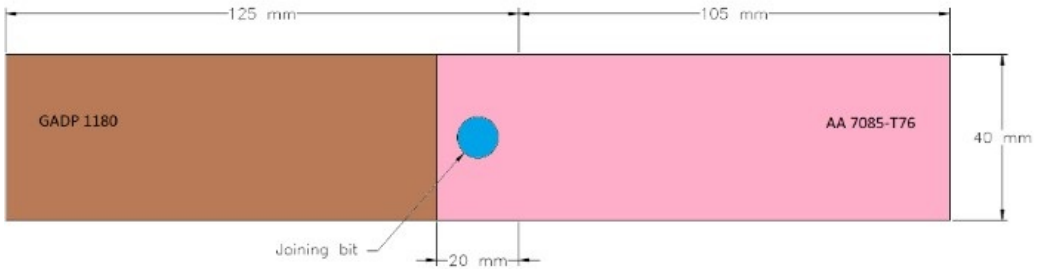


**Figure 3-11 Coupon Layout for Lap-Shear**

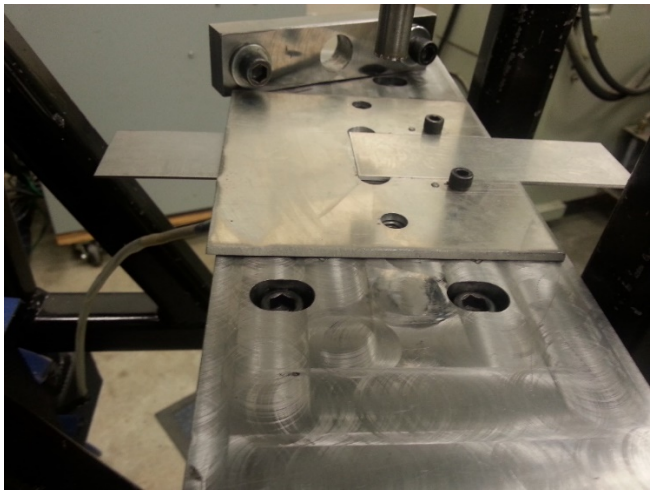

**Figure 3-12 Alignment Jig for Lap-Shear**

The specimens were tested using the same settings and outputs on the Instron machine as were used for the t-peel test. The specimens were placed in the machine with shims (steel shim against the aluminum coupon and an aluminum shim against the steel coupon) to align the sample pull direction perpendicular to the axis of the consumable bit (Figure 3-13).

**Figure 3-13 Shims to Align Coupons for Tension Testing**

### 3.7.4 Fatigue

The fatigue test was performed with the same specimens that were created for the lap-shear tests. Fatigue fracture is the most common form of failure for most engineering components(Zakaria, Abdullah et al. 2013). The Instron machine used for the fatigue test has the ability to oscillate a load at a fixed frequency for long periods of time. The specimens were placed in the machine and the load applied oscillated between 0.100 kN to 0.750 kN at a frequency of 20 Hz (Figure 3-14 and Figure 3-15). The requirement is that the sample holds for at least ten million cycles. The specimens were only tested till they passed the ten million cycles and then they were tested for lap-shear strength to evaluate if there was a loss of strength that occurred during the fatigue test.

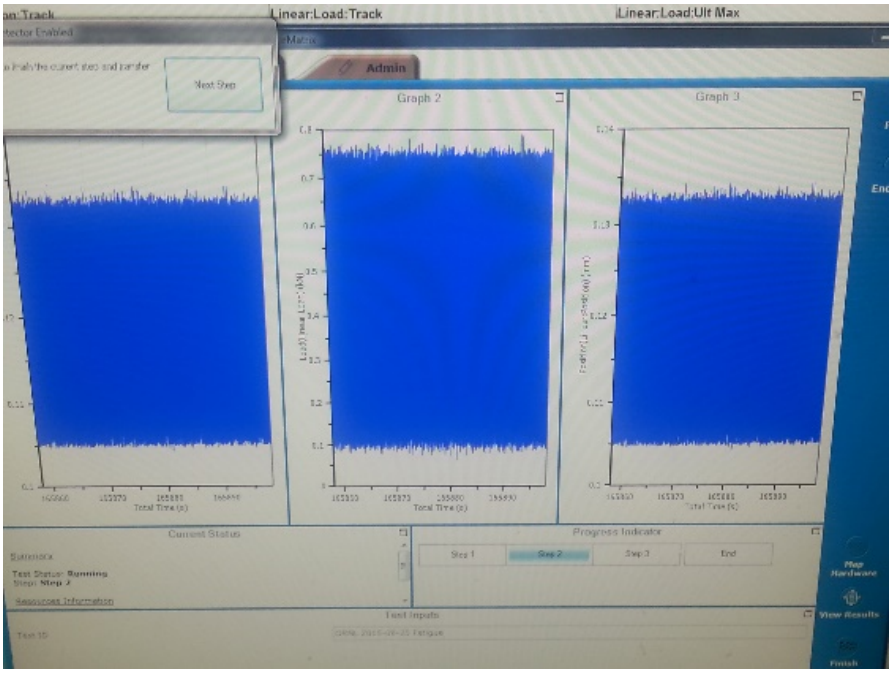


**Figure 3-14 Screen of Oscillating Loads for Fatigue Test**

**Figure 3-15 Instron Machine Running Fatigue Test**

### 3.7.5 Cross-Tension

The coupons for the cross tension are a different size from the coupons of the other tests, they are 150 mm x 50 mm. The coupons are placed crossing each other as shown in Figure 3-16 and welded in the center of the overlapping area. The welded specimens are placed in the Instron machine using a jig as shown in Figure 3-17 and pulled at the same rate as the other tests.

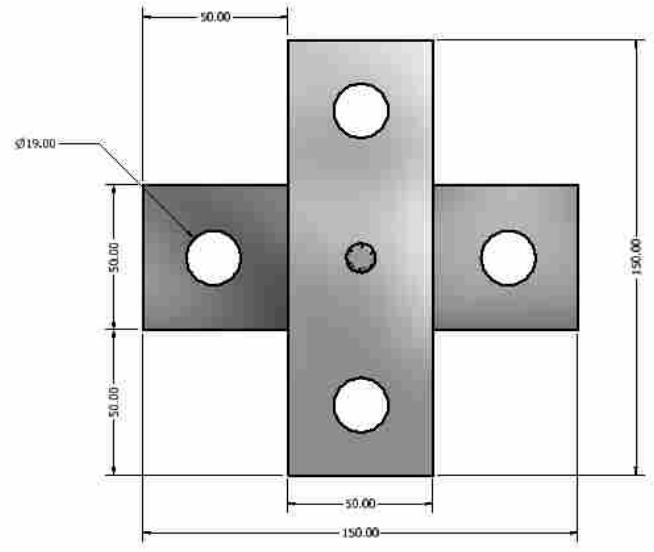


**Figure 3-16 Cross-Tension Layout**

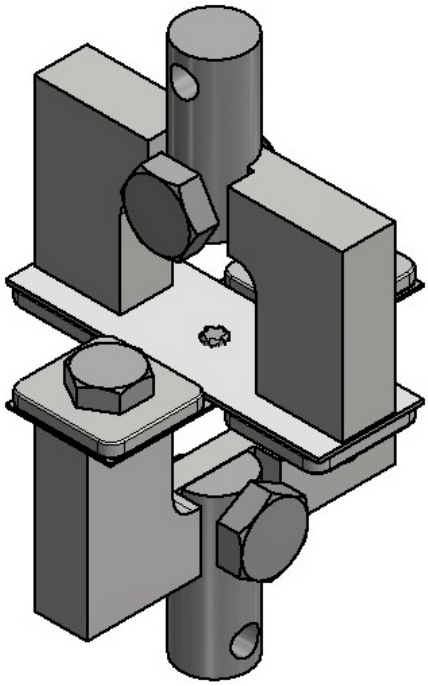

**Figure 3-17 Cross-Tension Jig**

### 3.7.6 Optical Microscopy Examination

Optical and electron microscopy examination was obtained by sectioning selected specimens based on weld parameters and bit material. The specimens were cut through the center of the consumable bit (Figure 3-18) using a wire EDM machine (Figure 3-19). A small sample was cut (Figure 3-20) out to be placed in plastic to form a puck for polishing and viewing (Figure 3-21).

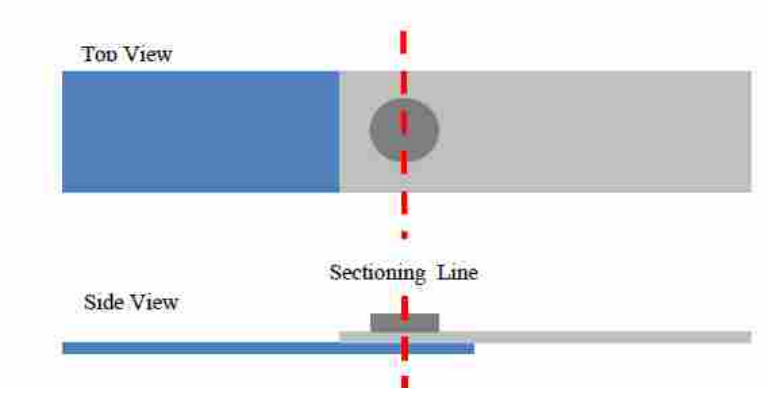


**Figure 3-18 Location of Sectioning Cut Path**

**Figure 3-19 Wire EDM Machine**

**Figure 3-20 Sample Cut on Wire EDM**

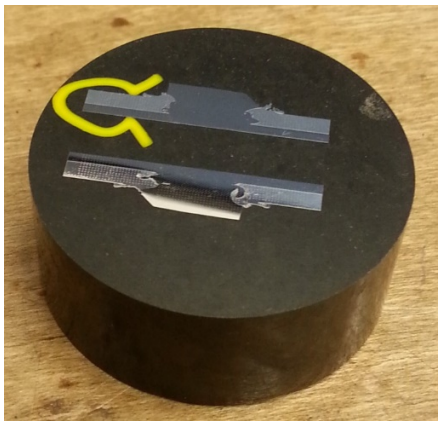

**Figure 3-21 Samples in Puck for Viewing**

# 4 RESULTS AND ANALYSIS

## 4.1 Bit Engineering and Properties

The bit required the ability to cut through the aluminum, remove the galvanic coating from the steel, and then create enough friction heat against the steel that a strong weld would form. In previous research the joint strength of the lap-shear layout was used as the standard. In this research we used the joint strength of the t-peel layout as the standard for evaluating the bit design and properties. After gaining sufficient strength in the t-peel joint to pass the minimum requirements, the other testing layouts were re-tested to confirm that they still achieved sufficient strength to pass the minimum requirements.

### 4.1.1 Bit Hardness

We found that the material hardness of the bit should be between 35 and 45 RC. If the bit was too "soft" or too "hard" the joint strength decreased. Tempering of the materials 4140, 4130, O1 tool steel, and 1018, achieved hardness within the desired range for all materials. Out of these four materials 1018 is the least expensive raw material and it is also the best for cold heading. Because of these properties and its ability to make strong welds (Section 4.5 T-Peel), 1018 became the material of choice. The tempering procedure required wrapping the 1018 bits in stainless steel foil with a small bit of paper to remove oxygen. We heated the bits to $1010^0$C

and soaked them at that temperature for 40 minutes. After the heat soak we had to cut the stainless steel foil and drop the bits in a water quench.

### 4.1.2 Bit Profile, Shaft Diameter and Cutting Features

The bits were produced using the Okuma CNC Lathe to create the cutting profile and then the top (external shape for driving) was created using cold forming. The Okuma was programed to shape the cutting profile. This profile evolved over time (Figure 4-1), starting with a short flute, no point ("nub") and small diameter progressing to a deeper flute, a guide "nub," and a larger diameter.

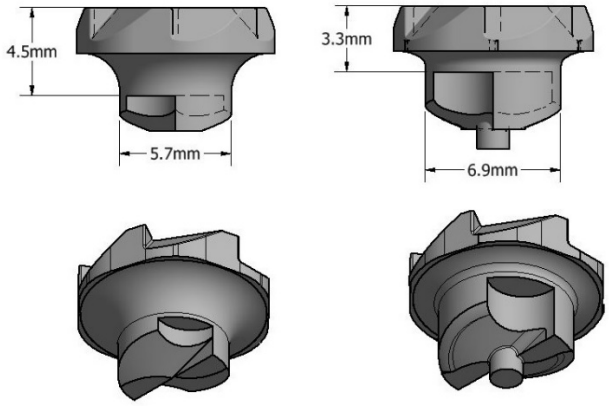


**Figure 4-1 Bit Evolution**

We found that the deeper flute was better at letting the aluminum out of the hole before the weld started. The larger diameter created a larger weld area which increased the strength of the FBJ but the standard deviation of the maximum loads achieved was close to 50% of the average maximum load. With the "nub" the consistency in the joint strength increased, reducing the standard deviation to less than 15% of the average maximum load (Table 9, Page 49).

## 4.2 Bit Driving Mechanism

A custom driver (Figure 4-2) was needed to hold the bit in place before starting the weld and spin the bit during the weld. A RAM EDM was used to create the correct shape in the driver end. Then a hole was drilled in the center to allow a magnet to be placed in it. The magnet holds the bit in place while the machine is starting the welding cycle. The final steps were putting a chamfer on the inside edge to allow the bit easier access and to machine out portions of the sides to create a cutting surface to assist in removing the aluminum flash.

**Figure 4-2 Driver with Bit**

## 4.3 Weld Microstructure

### 4.3.1 Viewing the Microstructure

We cut a sample weld through the middle of the weld and polished the cut edge (Section 3.7.6) to view under a microscope. We were able to understand more about the welding process as we viewed the different parts of the weld. As we increased the bit diameter the joining area also increased. When we added the deeper flutes there seemed to be less aluminum in the

welded area. When we added the "nub" to the bit there was a better bond area between the two metals. We hypothesized this was due to a better penetration of the bit into the AHSS. There seemed to be less (if any) voids in the weld area (Figure 4-3 and Figure 4-4).

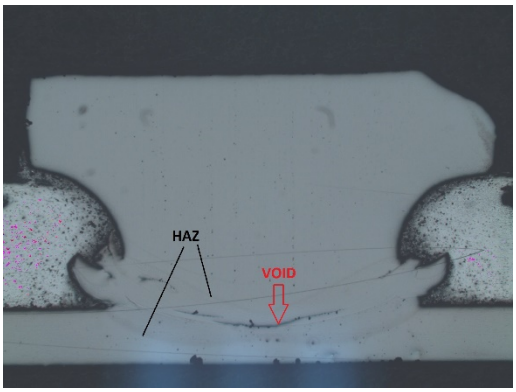


**Figure 4-3 Example of Void in Sectioned Weld**

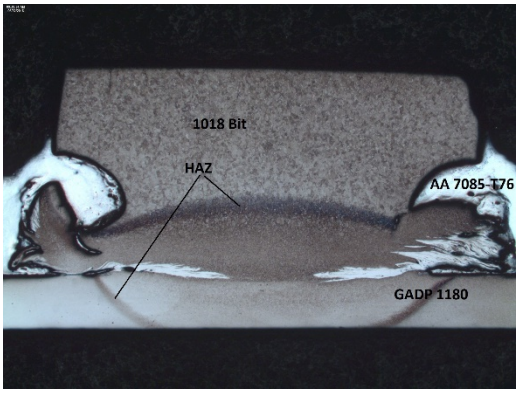


**Figure 4-4 Example of No Void in Sectioned Weld**

### 4.3.2 Measuring the Micro-Hardness

We measured the micro-hardness of sectioned samples to show how the welding process affects the hardness of the materials. From Figure 4-5 through Figure 4-8 we can see there is hardening due to the welding. The bits and the steel coupons in each sample started about the same hardness before the weld, which is shown by the coloring in figures below. For

consistency we set the hardness limits in our charts with a minimum of 20 HRC and a maximum of 50 HRC. Any points above 50 HRC are shown as 50 HRC and any points below 20 HRC are shown as 20 HRC in the figures below.

The “old style” bit shows less penetration in the weld than the “new style” bit. This is clear in all 4 of the figures but is most obvious in Figure 4-6 and Figure 4-8 which contain the coupons.

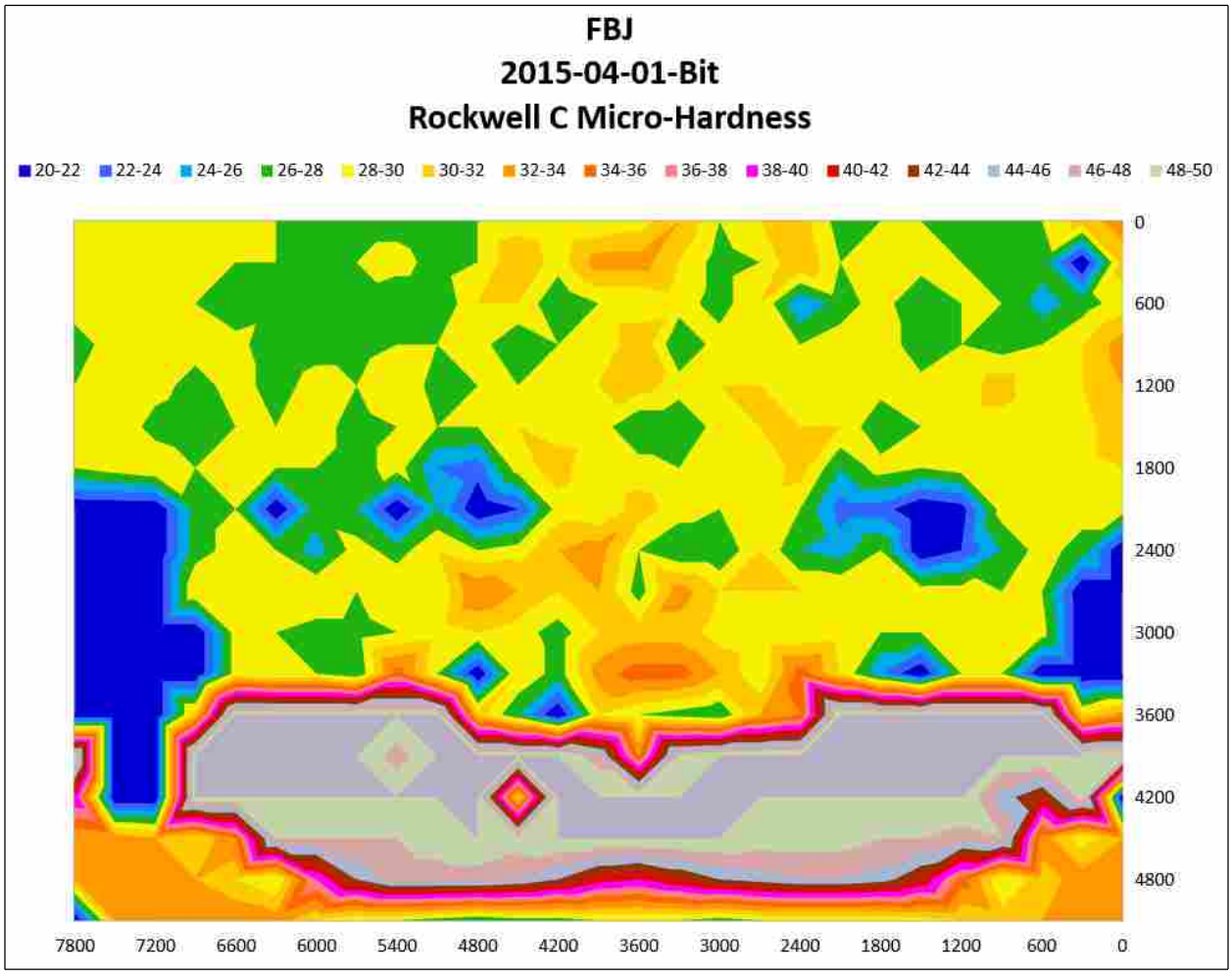


**Figure 4-5 Micro-Hardness 4140 Old Style Bit Welded to DP 980 (Showing Bit)**

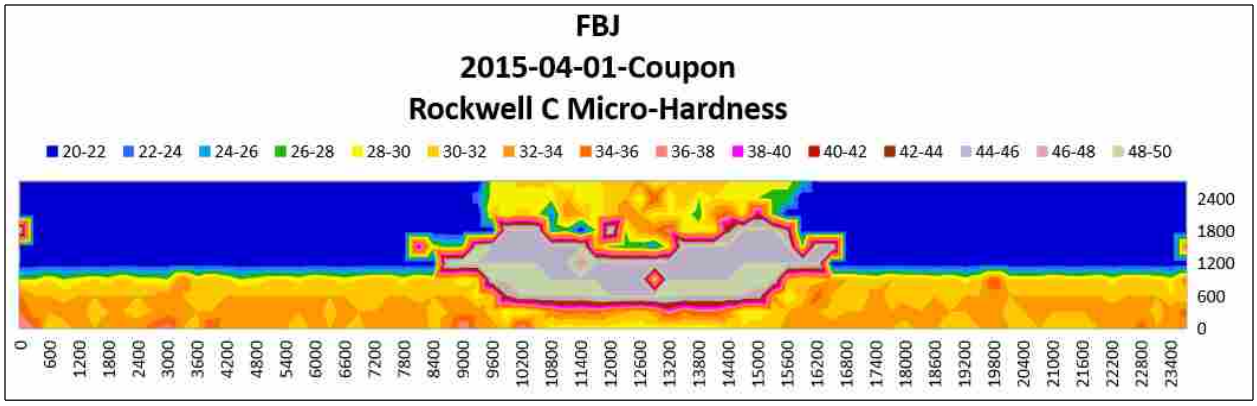


**Figure 4-6 Micro-Hardness 4140 Old Style Bit Welded to DP 980 (Showing Coupons and Bit)**

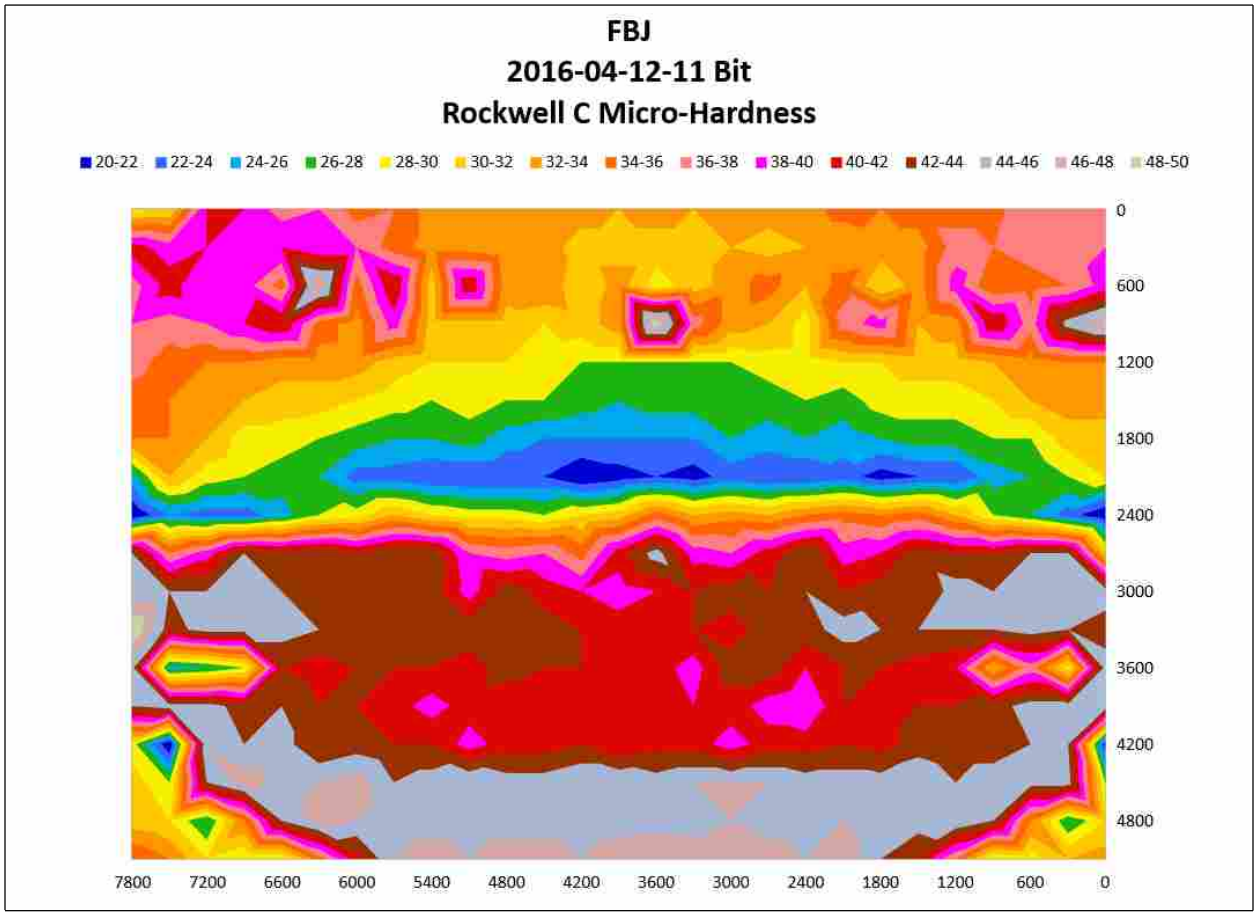


**Figure 4-7 Micro-Hardness 1018 New Style Bit Welded to GADP 1180 (Showing Bit)**

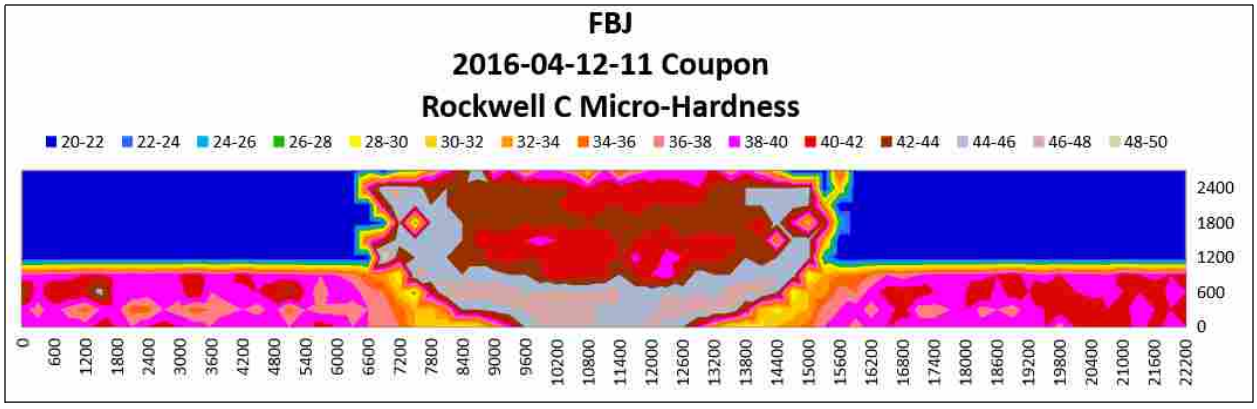


**Figure 4-8 Micro-Hardness 1018 New Style Bit Welded to GADP 1180 (Showing Coupons and Bit)**

## 4.4 Failure Modes

We experienced three failure modes while testing the FBJ joints: nugget (Figure 4-9 and Figure 4-10); material (Figure 4-13); and interfacial (Figure 4-15).

### 4.4.1 Nugget Failure Mode

Nugget failure occurs when a nugget of steel tears out during the test. The nugget could form as a small round pullout (Figure 4-9) or the steel could tear in a longer strip (Figure 4-10). Nugget pullout failure is the most desirable failure because the joints that fail in nugget pullout are assumed to have better energy absorption(Marya and Gayden 2005)(Table 9 Page 49). The charts in Figure 4-11, Figure 4-12, Figure 4-14, and Figure 4-16 show greater extension was achieved during the tests with nugget failure mode than any other failure mode. The extension for a nugget failure requires a load to be held for much longer while it tears the steel, thus requiring more energy before failure with the same maximum load compared to other failure modes.

During the weld, heat is generated creating a HAZ (heat affected zone). The material in the HAZ area is tempered and softened creating a region more susceptible to failure(Marya and Gayden 2005). This in turn creates a situation where nugget pullout is possible. With the final bit design, for this research, the nugget pullout failure happened over 88% of the time (Table 9 shows 15 out of 17 samples). Table 9 also shows the work in joules, or the energy absorbed, to break the FBJ bond. All nugget failures absorbed substantially more energy than the interfacial failures.

**Figure 4-9 Nugget Joint Failure Small Steel Tear**

**Figure 4-10 Nugget Joint Failure Large Steel Tear**

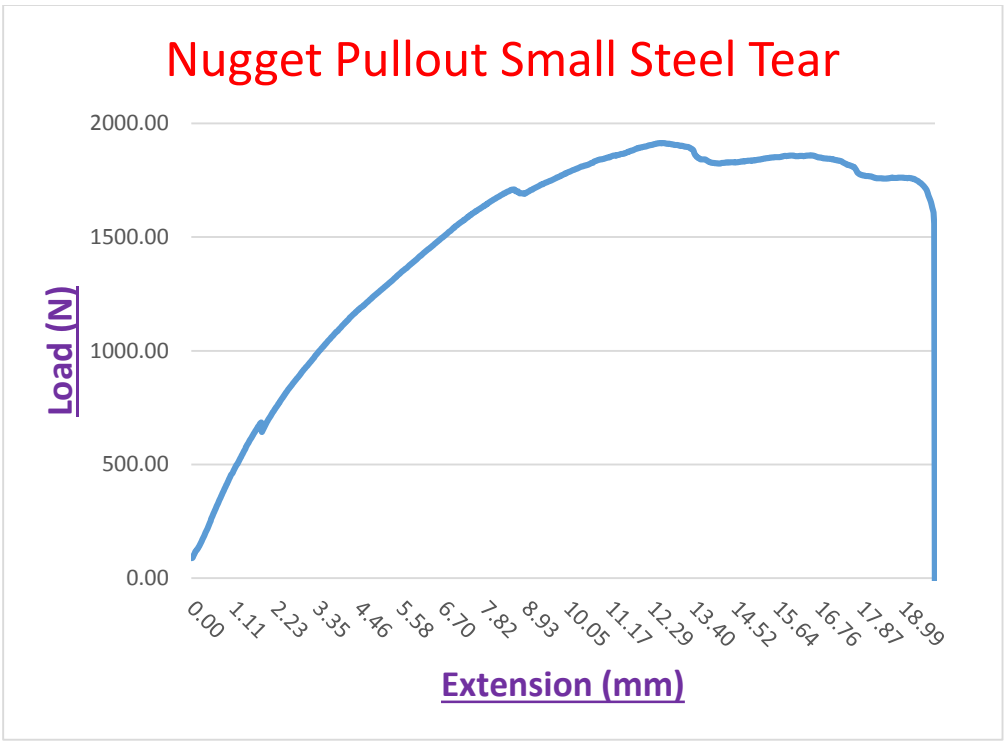


**Figure 4-11 Load vs. Extension for Nugget Small Steel Tear**

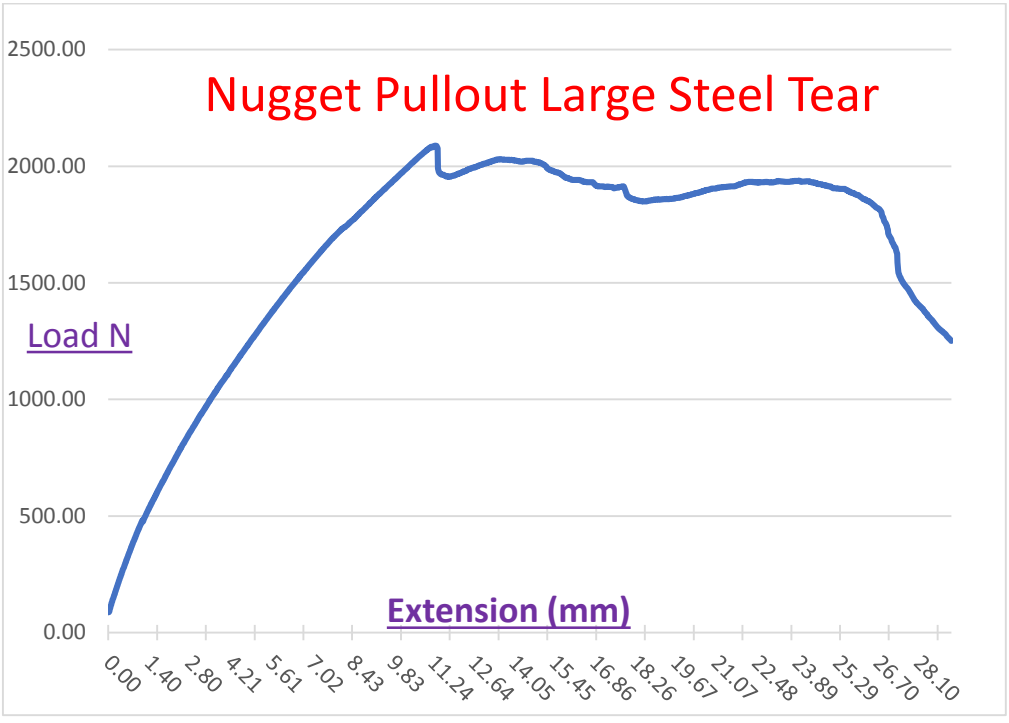


**Figure 4-12 Load vs. Extension for Nugget Large Steel Tear**

### 4.4.2 Material Failure Mode

Material failure is characterized by the bit and weld staying intact while the coupons separate because the softer material reached its ultimate tensile strength (UTS) (Figure 4-13). During the t-peel testing this only happened if the driver touched the base material of the coupon when cleaning the aluminum flash, thus creating a bit head that was slightly counter sunk into the aluminum. This reduced the thickness of aluminum holding against the bit head and the overall strength of the coupon at the head location.

**Figure 4-13 Material Joint Failure**

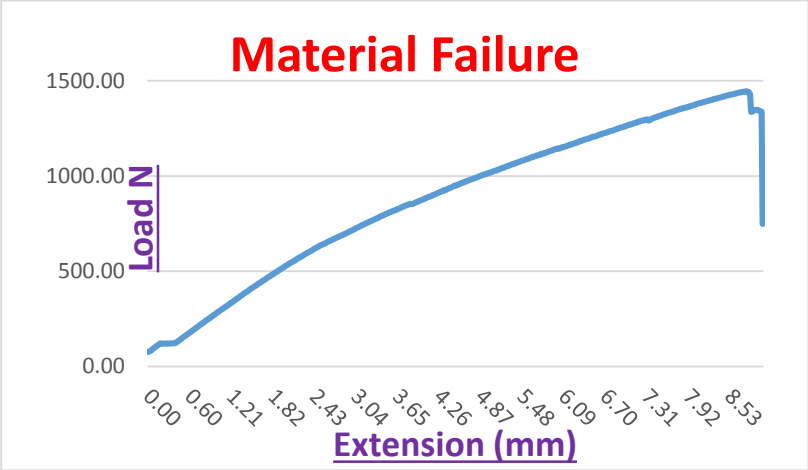


**Figure 4-14 Load vs. Extension for Material Failure**

### 4.4.3 Interfacial Failure Mode

Interfacial is the least desirable failure, because it absorbs the least amount of energy to failure. With an interfacial failure the bit material can be observed in both of the coupon samples (Figure 4-15). The materials separate at the interface between the two coupons. There can also be a combination of interfacial and nugget pullout.

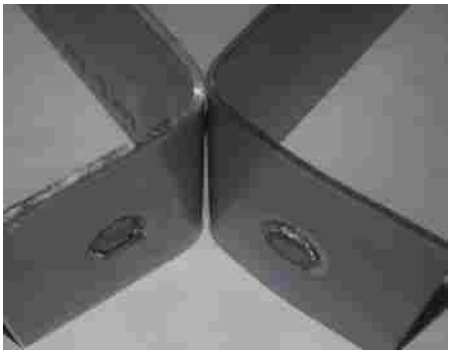

**Figure 4-15 Interfacial Joint Failure**

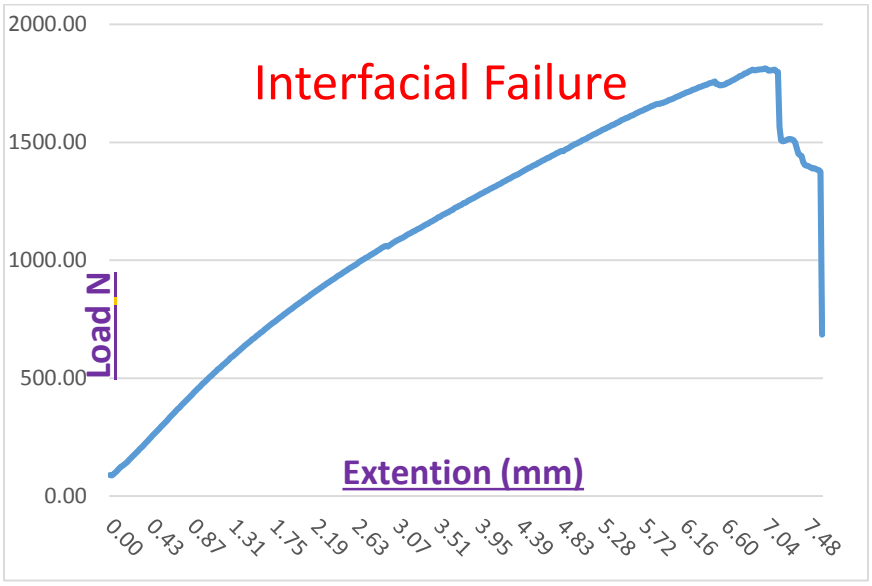


**Figure 4-16 Load vs. Extension for Interfacial Failure**

## 4.5 T-Peel

T-peel testing is the most severe of all the tests performed during this research. It is very important because it is the test that is used to evaluate crash worthiness for automotive applications. This test is also the only test that previous research was not able to achieve the required joint strength. When we started doing the t-peel test we found that the joint strength was well below the standards for automotive applications.

While bending the coupons the outer structure of the material is in tension while the inner structure is in compression. As the bending radius decreases the tensile load increases. This tensile load can cause the material to fail. This failure was experienced until we changed the procedure for bending the coupons as discussed in Section 3.7.2 T-Peel Test.

The automotive standard for t-peel failure is 1.5kN. The early testing for t-peel returned poor results (Table 4). The average peak load was 350 N about 23% of the required standard.

**Table 4 Early T-Peel Results**

| 4140 BH - 5.7mm diameter | | | |
|---|---|---|---|
| T peel tests | | | |
| count | Sample # | Hardness RC | Peak Load N |
| 1 | 2015-05-13-04 | 25-30 | 322 |
| 2 | 2015-05-13-05 | 25-30 | 265 |
| 3 | 2015-05-13-06 | 25-30 | 298 |
| 4 | 2015-05-13-07 | 25-30 | 393 |
| 5 | 2015-05-13-08 | 25-30 | 473 |

### 4.5.1 Heat Treating Bits

We heated 6 small cylindrical samples of 4140 bit material to $845^0$C and "soaking" for 45 minutes in a stainless steel foil pouch (to keep the oxygen away from the bit material while heating). The cylindrical samples were used, rather than actual bits, to assist in measuring the HRC hardness. After the samples were quenched in oil they were removed from the pouch and re-heated to $630^0$C, one sample was removed every 30 minutes tempering them. Only the samples that were not re-heated increased in hardness, all other samples were in the same range as the untreated material. We repeated the process but removed samples every 5 minutes during the tempering process. This provided samples with hardness of: no tempering at 50 HRC; 5 minutes at 38 HRC; 10 minutes at 36 HRC; 15 minutes at 34 HRC; 20 minutes at 32 HRC; and 25 minutes at 30 HRC. We heat treated the bits in groups of 5 for the first 3 hardness levels. The joint strength (peak load values) remained similar to previous tests.

We followed similar procedures with the other bit material to achieve a hardness between 35 HRC and 45HRC. The 1018 required water quenching and no re-heating to achieve the desired hardness.

### 4.5.2 Changing Machine Settings

The microstructure of the weld (Section 4.3 Weld Microstructure) showed that the bit did not penetrate into the steel. We wanted to achieve better penetration into the steel to increase the strength of the joint. To achieve this we hypothesized that keeping the bit cool as it cut through the aluminum would allow the bit to scratch the steel before it started softening. We reduced the spindle speed for the cutting stage to 800 RPM, leaving the welding spindle speed at 2500RPM.

This increased both the average maximum and the standard deviation for the joint strengths (Table 5).

**Table 5 Spindle Speed Adjustment T-Peel Results**

| 4140 Bit 800 RPM Cutting Speed Welded to DP980 | | | |
|---|---|---|---|
| T peel tests | | | |
| count | Sample # | Hardness RC | Peak Load N |
| 1 | 2015-06-23-00 | 25-30 | 448 |
| 2 | 2015-06-23-01 | 25-30 | 504 |
| 3 | 2015-06-23-02 | 25-30 | 444 |
| 4 | 2015-06-23-03 | 25-30 | 1098 |
| 5 | 2015-06-23-04 | 25-30 | 452 |
| | | AVG | 589 |
| | | STD | 285 |

Other changes to the spindle speed for cutting through the aluminum did not improve the results using the old bit design and material. We adjusted the plunge depth of the weld cycle and found no improvements. We added a dwell into a stage between the cutting stage and the welding stage, the results started improving a little. We adjusted the dwell between 100 and 500 milliseconds and reduced the spindle speed during the dwell to 500RPM. These changes allowed us to break the minimum requirements inconsistently, but the minimum values kept the averages close to the same as before (Table 6).

**Table 6 T-Peel Results with 500 ms Dwell**

| 4140 Bit with 500 ms Dwell Welded to DP980 | | | |
|---|---|---|---|
| T peel tests | | | |
| Count | Sample # | Hardness RC | Peak Load N |
| 1 | 2015-07-13-00 | 25-30 | 233 |
| 2 | 2015-07-13-01 | 25-30 | 419 |
| 3 | 2015-07-13-02 | 25-30 | 297 |
| 4 | 2015-07-13-03 | 25-30 | 250 |
| 5 | 2015-07-13-04 | 25-30 | 275 |
| 6 | 2015-07-13-05 | 25-30 | 1733 |
| | | AVG | 535 |
| | | STD | 591 |

### 4.5.3 Bit Materials and Design

We purchased different materials for bit manufacture and compared the joint strength that each bit material could create. There were 2 reasons for trying new bit material; the first was to see if we could get a better weld penetration into the steel, the second was to reduce the cost of the bit material. We wanted a material that can be held into the driver with a magnet, and we wanted it to be in the 25-30 HRC range to match the hardness of the DP 980. We purchased O1 tool steel that matched this criteria. The results were not an improvement (Table 7) so we continued to look for new materials.

**Table 7 O1 Tool Steel Bit**

| O1 Tool Steel Bit Welded to DP980 | | | |
|---|---|---|---|
| T peel tests | | | |
| count | Sample # | Hardness RC | Peak Load N |
| 1 | 2015-10-09-03 | 25-30 | 217 |
| 2 | 2015-10-09-03 | 25-30 | 205 |
| 3 | 2015-10-09-03 | 25-30 | 483 |
| 4 | 2015-10-09-03 | 25-30 | 361 |
| 5 | 2015-10-09-03 | 25-30 | 220 |
| 6 | 2015-10-09-03 | 25-30 | 397 |

We purchased some 4130 and 1018 steels to try as bits. We made no effort to modify the hardness of the materials, we just used them as is. The 4130 was in the hardness range we were looking for, between 25-30 HRC; while the 1018 was much softer but was substantially less expensive. The 4130 produced the best results using the adjusted welding parameters (Table 8).

**Table 8 Three Bit Material Comparison**

| 3 material comparison<br>Webbed to DP980<br>T peel tests | | | |
|---|---|---|---|
| count | Sample # | Material | Peak Load N |
| 1 | 2015-11-20-06 | 4140 | 1395 |
| 2 | 2015-11-20-01 | 4140 | 1425 |
| 3 | 2015-11-20-02 | 4140 | 1060 |
| 4 | 2015-11-20-03 | 4140 | 1736 |
| 5 | 2015-11-20-04 | 4140 | 1713 |
| 6 | 2015-11-20-05 | 1018 | 462 |
| 7 | 2015-11-20-06 | 1018 | 339 |
| 8 | 2015-11-20-07 | 1018 | 490 |
| 9 | 2015-11-20-08 | 1018 | 588 |
| 10 | 2015-11-20-09 | 1018 | 229 |
| 11 | 2015-11-20-10 | 4130 | 1919 |
| 12 | 2015-11-20-11 | 4130 | 1870 |
| 13 | 2015-11-20-12 | 4130 | 1711 |
| 14 | 2015-11-20-13 | 4130 | 652 |
| 15 | 2015-11-20-14 | 4130 | 2010 |

The automotive sponsor changed coupon materials and sizes at this point. 40mm x 125mm with the aluminum AA 7085 T75 and the steel GADP1180. The change in the aluminum made little difference, we ran tests with the old steel DP980 and the welds worked the same. The galvanized surface on the new steel seemed to prevent the friction weld from working, we ran some tests with non-galvanized DP1180 and the test results were similar and a little stronger than the previous materials. We hypothesized the galvanic coating was not allowing enough heat to build up in the short weld time. We started heat treating the bits again to increase the hardness of the bit enough to scratch off this coating. We found that a hardness between 35 and 45 HRC created welds again. Using the 3 different materials we found that similar joint strengths were reached for all materials. 1018 is significantly less expensive than the other 2 materials and it is

also cold formable which lowers the price for production. We refined the bit design, illustrated on the left in Figure 4-1, to the design that is shown on the right in Figure 4-1. With the new bit design, and using 1018 hardened steel for the bits (as described in section 4.1.1.) we were able to obtain consistent passing results. The passing results as well as elongation to failure and the work required to achieve failure are shown in Table 9. An example of the work calculation using weld sample 2016-04-29-05 for the adhesive work to failure is shown in appendix A.

**Table 9 T-Peel Results - 1018 Bit Material**

| 1018 Bits with "Nub" | | | | | | |
|---|---|---|---|---|---|---|
| T peel tests machine settings<br>Stage 1 – 4000 RPM, z velocity 28 ipm, z depth -0.127", 50 ms dwell<br>Stage 2 – 4000 RPM, z velocity 4.5 ipm, z depth -0.232" | | | | | | |
| ccnt0 | Sample # | Hardness RC | Failure Mode | Peak Load N | Elongation mm | Work J |
| 1 | 2016-04-12-08 | 38 | Nugget | 1656 | 15.3 | 14.6 |
| 2 | 2016-04-12-09 | 38 | Nugget | 2087 | 29.81 | 48.1 |
| 3 | 2016-04-12-10 | 38 | Nugget | 1624 | 15.6 | 18.4 |
| 4 | 2016-04-12-12 | 45 | Nugget | 1675 | 15.41 | 18.3 |
| 5 | 2016-04-12-13 | 45 | Nugget | 1675 | 15.8 | 19.8 |
| 6 | 2016-04-12-14 | 45 | Nugget | 1711 | 16.9 | 21.5 |
| 7 | 2016-04-[S-06] | 45 | Nugget | 1900 | 24.5 | 32.3 |
| 8 | 2016-04-[S-01] | 45 | Nugget | 1713 | 15.1 | 19.0 |
| 9 | 2016-04-[S-02] | 45 | Nugget | 1794 | 23.5 | 33.5 |
| 10 | 2016-04-[S-03] | 38 | Nugget | 2053 | 25.1 | 41.5 |
| 11 | 2016-04-[S-04] | 38 | Nugget | 1740 | 13.7 | 17.1 |
| 12 | 2016-04-[S-05] | 38 | Nugget | 2004 | 20.9 | 32.8 |
| 13 | 2016-04-[S-06] | 45 | Nugget | 1921 | 24.5 | 38.3 |
| 14 | 2016-04-[S-07] | 44 | Interfacial | | 4.6 | 3.5 |
| 15 | 2016-04-[S-08] | 44 | Interfacial | 1814 | 7.6 | 8.0 |
| 16 | 2016-04-[S-09] | 44 | Nugget | 2136 | 28.1 | 45.9 |
| 17 | 2016-04-[S-10] | 44 | Nugget | 1914 | 19.8 | 29.7 |

## 4.6 Lap-Shear Tension

The main failure mode experienced in this research for the lap-shear tension test was material failure (Figure 4-17). In previous research interfacial was the most common. A possible cause for this change in failure mode is the change in coupon layout. The overlapping surface in previous research was 25mm. The standards for the overlapping surface were changed during this research to 20mm, this was part of the change in coupon size. This change allows less material to resist the pressures applied during the tension testing and therefore increases the chances of material failures. The average failure load was lower (Table 10) in this research than in previous research but still well above minimum requirements. We believe that the lower shear loads were also caused by the change in the coupon layout and not the FBJ. Very few of the welds failed during these tests where as in previous research most of the welds failed.

**Table 10 Lap-Shear Test Data**

| 1018 Bits with "Nub" | | | | | |
|---|---|---|---|---|---|
| Lap-Shear tests machine settings<br>Stage 1 – 4000 RPM, z velocity 28 ipm, z depth -0.127", 50 ms dwell<br>Stage 2 – 4000 RPM, z velocity 4.5 ipm, z depth -0.232" | | | | | |
| Count | Sample # | Failure Mode | Peak Load kN | Total Elongation mm | Total Work (J) |
| 1 | 2016-04-13-00 | Material | 10.0 | 4.74 | 35 |
| 2 | 2016-04-13-02 | Material | 7.4 | 3.48 | 22.6 |
| 3 | 2016-04-13-03 | Mat/Int | 7.8 | 2.01 | 9.8 |
| 4 | 2016-04-13-04 | Material | 8.9 | 4.76 | 33.8 |

**Figure 4-17 Lap-Shear Material failure**

## 4.7 Cross-Tension

The cross-tension test is more severe than the lap-shear test but not as severe as the t-peel. In previous testing at BYU cross-tension specimens were made using different weld parameters and bit design than those used in the current study. In this study we only did the cross-tension testing after the t-peel had passed minimum requirements. The average tensile strength for five cross-tension experiments in the previous research was found to be 2.88kN(Squires 2014). The current research results are given in Table 11. The average tensile strength for five cross-tension experiments was found to be 4.9kN. Three of the experimental failures were interfacial and two were nugget pullout (Figure 4-18).

**Table 11 Cross-Tension Data**

| 1018 Bits with "Nub" | | | | | |
|---|---|---|---|---|---|
| Cross-Tension tests machine settings<br>Stage 1 – 4000 RPM, z velocity 28 inm, z depth -0.127", 50 ms dwell<br>Stage 2 – 4000 RPM, z velocity 4.5 inm, z depth -0.232 | | | | | |
| Count | Sample # | Failure Mode | Peak Load N | Total Elongation mm | Total Work - in |
| 1 | 2016-05-11-00 | Interfacial | 3548.0 | 1.418 | 19.8 |
| 2 | 2016-05-11-01 | Interfacial | 5204.0 | 0.149 | 24.5 |
| 3 | 2016-05-11-02 | Interfacial | 4047.0 | 1.647 | 33.8 |
| 4 | 2016-05-11-03 | Nugget | 5609.0 | 0.791 | 39.9 |
| 5 | 2016-05-11-04 | Nugget | 6045.0 | 0.95 | 44.8 |

**Figure 4-18 Cross-Tension with Nugget and Interfacial Failures**

## 4.8 Fatigue Tension

For automotive applications fatigue testing is very important. The specimens for this research were allowed to run the minimum ten million cycles at 20Hz. If there was no failure before the end of the test then the specimens were subjected to a lap-shear test to see how strong the joint was after finishing the fatigue cycles. We experienced no failure during the fatigue testing and all samples exceeded the minimum required loading during the lap-shear testing after ten million cycles in the fatigue test.

## 4.9 Adhesive Weld Bonding and FBJ

We were supplied with adhesives from two different suppliers which will be referred to as "Adhesive A" and "Adhesive B". These adhesives were tested in conjunction with the FBJ.

### 4.9.1 Weld Bond T-Peel

With the combination of adhesive and FBJ each welded sample failed twice. Since the FBJ allows for elongation before failure the first failure was at the point where the adhesive failed and the second failure was at the point where the FBJ failed. For the adhesives failure the extension at break ranges from .25mm to 1.00mm. This small amount of extension is not enough

to apply sufficient load to the FBJ for it to break. Therefore there was a peak load at the adhesive break and then the load drops as the adhesive lets go of the coupons allowing a smaller load to transfer to the FBJ. We started the loading again to find the peak load for the FBJ break. We did not find a correlation between the adhesive strength and the FBJ strength (Table 12 and Table 13). Even though the adhesive part of the weld/bond joint may be stronger there is substantially more elongation occurring during the FBJ failure. Since the elongation happens under load it takes more work (or energy) to break the FBJ than it does to break the adhesive. The work was approximated by multiplying the load at each data point collected (10 points were collected per second) with the change in elongation between that point and the previous point, and adding the work energy of each calculation to the energy of the last calculation. These calculations supply an approximate total work for the joint at the last sample.

**Table 12 Weld Bond Adhesive A T-Peel Test**

| Weld Bonded Adhesive A T peel tests | | | | | | | | |
|---|---|---|---|---|---|---|---|---|
| | | | Adhesive Failure | | | FBJ Failure | | |
| Count | Sample # | FBJ Failure Mode | Adhesive Peak Load N | Total Elongation mm | Work J | FBJ Peak Load N | Total Elongation mm | Work J |
| 1 | 20160404-2nd05 | Nugget | 1353 | 10.45 | 0.45 | 1727 | 16.74 | 23.24 |
| 2 | 20160404-2nd06 | Nugget | 1666 | 10.58 | 0.57 | 2016 | 22.02 | 35.32 |
| 3 | 20160404-2nd07 | Nugget | 1570 | 10.55 | 0.56 | 2058 | 30.13 | 51.60 |
| 4 | 20160404-2nd08 | Nugget | 1628 | 10.38 | 0.38 | 2038 | 27.40 | 47.52 |
| 5 | 20160404-2nd09 | Nugget | 1346 | 10.40 | 0.40 | 1710 | 12.56 | 14.96 |

**Table 13 Weld Bond Adhesive B T-Peel Test**

| Weld/Bonded Adhesive B | | | | | | | | |
|---|---|---|---|---|---|---|---|---|
| T peel tests | | | | | | | | |
| | | | Adhesive Failure | | | FBJ Failure | | |
| count | Sample # | FBJ Failure Mode | Adhesive Peak Load N | Total Elongation mm | Work (J) | FBJ Peak Load N | Total Elongation mm | Work (J) |
| 1 | 2016-04-29-00 | Interfacial - Nugget | 3093 | 0.93 | 1.89 | 1661 | 10.20 | 10.89 |
| 2 | 2016-04-29-01 | Interfacial | 3445 | 0.90 | 1.93 | 1422 | 5.34 | 4.68 |
| 3 | 2016-04-29-02 | Nugget | 3495 | 1.04 | 2.20 | 2024 | 51.22 | 87.92 |
| 4 | 2016-04-29-03 | Nugget | 3411 | 0.97 | 2.05 | 2011 | 25.92 | 42.60 |
| 5 | 2016-04-29-04 | Interfacial | 3212 | 0.96 | 1.86 | 724 | 2.53 | 0.95 |

### 4.9.2 Weld Bond Lap-Shear

When we compared failure modes for the FBJ without adhesive and the FBJ with adhesive for the lap-shear test, we found less material failures for the weld/bond samples. Table 14 and Table 15 show the failure modes for the weld/bond samples which were: 5 material failures; 3 interfacial failures; and 1 nugget pullout. Only sample 2016-05-16-15 experienced a double failure between the adhesive and the FBJ, the second pull yielded 12.5kN and a nugget pullout failure. The adhesive seems to increase the ability of the material to withstand the loads applied by the joint during testing. The results exceed the requirements.

**Table 14 Weld Bond Adhesive A Lap-Shear**

1018 Bits with "Nub" Weld Bond Adhesive A

Lap-Shear tests machine settings
Stage 1 – 4000 RPM, z velocity 28 ipm, z depth -0.127", 50 ms dwell
Stage 2 – 4000 RPM, z velocity 4.5 ipm, z depth -0.232

| Count | Sample # | Failure Mode | Peak Load kN | Total Elongation mm | Total Work J |
|---|---|---|---|---|---|
| 1 | 2016-05-20-01 | Interfacial | 12.3 | 26 | 21.6 |
| 2 | 2016-05-20-01 | Nugget | 13.5 | 28 | 26.8 |
| 3 | 2016-05-20-02 | Material | 14.4 | 32 | 30.7 |
| 4 | 2016-05-20-03 | Interfacial | 14.4 | 25 | 21.8 |
| 5 | 2016-05-20-04 | Interfacial | 12.7 | 30 | 23.4 |

**Table 15 Weld Bond Adhesive B Lap-Shear**

1018 Bits with "Nub" Weld Bond Adhesive B

Lap-Shear tests machine settings
Stage 1 – 4000 RPM, z velocity 28 ipm, z depth -0.127", 50 ms dwell
Stage 2 – 4000 RPM, z velocity 4.5 ipm, z depth -0.232

| Count | Sample # | Failure Mode | Peak Load kN | Total Elongation mm | Total Work J |
|---|---|---|---|---|---|
| 1 | 2016-05-16-11 | Material | 20.2 | 27 | 29.5 |
| 2 | 2016-05-16-12 | Material | 20.5 | 32 | 32.1 |
| 3 | 2016-05-16-13 | Material | 20.8 | 32 | 32.4 |
| 4 | 2016-05-16-14 | Interfacial | 23.3 | 53 | 37.4 |
| 5 | 2016-05-06-15 | Nugget | 23.8 | 105 | 60.4 |

### 4.9.3 Weld Bond Cross-Tension

For the cross-tension the adhesive did not seem to change the failure modes when compared with the FBJ only joints. These tests responded more like the adhesive t-peel test with two different failures measured. Table 16 and Table 17 show each of these failures. The first peak load is where the adhesive failed and the second is where the FBJ failed. Note that like the t-peel there is more work on average required to break the FBJ than the adhesive.

**Table 16 Weld Bond Adhesive A Cross-Tension**

| 1018 Bits with "Nub" Weld-Bond Adhesive A<br>Cross-Tension tests machine settings<br>Stage 1 – 4000 RPM, z velocity 28 ipm, z depth -0.127", 50 ms dwell<br>Stage 2 – 4000 RPM, z velocity 4.5 ipm, z depth -0.232 | | | | | | |
|---|---|---|---|---|---|---|
| Count | Sample # | Failure Mode | Peak Load 1 | Total Work (J) | Peak Load 2 | Total Work (J) |
| 1 | 2016-05-16-06 | Interfacial | 2667 | 7.1 | 5765 | 36.2 |
| 2 | 2016-05-16-07 | Nugget | 1834 | 2.9 | 6103 | 44 |
| 3 | 2016-05-16-08 | Material | 1823 | 2.9 | 5062 | 33.4 |
| 4 | 2016-05-16-09 | Nugget | 2453 | 6.2 | 6632 | 45.7 |
| 5 | 2016-05-16-10 | Interfacial | 2463 | 5.7 | 2943 | 8.8 |

**Table 17 Weld Bond Adhesive B Cross-Tension**

| 1018 Bits with "Nub" Weld-Bond Adhesive B<br>Cross-Tension tests machine settings<br>Stage 1 – 4000 RPM, z velocity 28 ipm, z depth -0.127", 50 ms dwell<br>Stage 2 – 4000 RPM, z velocity 4.5 ipm, z depth -0.232 | | | | | | |
|---|---|---|---|---|---|---|
| Count | Sample # | Failure Mode | Peak Load 1 | Total Work (J) | Peak Load 2 | Total Work (J) |
| 1 | 2016-05-16-00 | Interfacial | 6056 | 17.2 | 3351 | 8 |
| 2 | 2016-05-16-02 | Material | 5249 | 15.1 | 4126 | 21.5 |
| 3 | 2016-05-16-03 | Nugget | 5413 | 15.9 | 5849 | 35.7 |
| 4 | 2016-05-16-04 | Nugget | 5983 | 22.3 | 5836 | 34 |
| 5 | 2016-05-16-05 | Interfacial | 5151 | 16.5 | 793 | 0.6 |

# 5 CONCLUSIONS AND RECOMMONDATIONS

## 5.1 Conclusions

This research explored three hypotheses validating that FBJ is a viable method for joining advanced high-strength steels and aluminum.

Hypothesis 1 –

> FBJ can create a spot joint between galvanized DP 1180 steel and AA 7085-T76, where the strength exceeds minimum standards in lap-shear, cross-tension, fatigue, and t-peel configurations.

This research modified the cutting area of the bit design and changed the welding parameters to achieve passing results. In this research we have shown that FBJ can exceed minimum strength requirements for all of the standard tests. Creating the situation where the t-peel test could pass the standards was the main focus of this research. Through mechanical destructive testing and microstructure evaluation the welding parameters including bit design were analyzed and then modified to improve results. The results of this research do not reject this hypothesis.

Hypothesis 2 –

> A low carbon steel alloy, like 1018, can be used for the bit material in order to create joints of acceptable strength between galvanized DP 1180 and AA 7085-T76.

With the modified bit design and heat treatment of the 1018 bits we were able to achieve joints of acceptable strength for the required coupon materials. This research implies that when comparing material and hardness the hardness is more important. If another material is found to be better for mass production of the bits there is a high probability that given sufficient hardness and similar compatibility to the steel coupons it could work as a bit material. The research does not reject hypothesis number two.

Hypothesis 3 –

> A FBJ with this material combination can achieve the desired nugget pull out failure mode 100% of the time.

Nugget failure occurs when a nugget of steel tears out during the test. Nugget pullout failure is the most desirable failure because the joints that fail in nugget pullout have better energy absorption. Even though this research rejected the 100% nugget pullout mode there was a large improvement in failure modes. Because the failure mode is related to the amount of energy that the joint dissipates before failure, the failure mode was important to this research. The micro hardness testing done in this research showed how the nugget failure mode increased from previous research by comparing a sample created early in the research with a sample from our final bit design. The old bit design did not generate enough energy to allow the HAZ to penetrate through the steel coupon (Figure 4-6). The new bit design does (Figure 4-8). With the deeper, wider HAZ, there is a stronger bond between the steel coupon and the bit. The weaker zone is now in the steel coupon which allows nugget pullout to be a more prevalent failure mode.

The failure modes for three out of four tests occurred as follows: (1) for the lap-shear we had 100% material failure. This could be caused by the coupon sizes and layout but will require further research to confirm. Material failure was better than the previous researches interfacial

failure modes. (2) For the cross-tension we had about 40% nugget pullout failure. The joint strength was increased and the failure modes improved substantially from what was found in the previous research. (3) For the t-peel we had 88% nugget pullout failure. Achieving 88% nugget failure was a massive improvement from the previous research. There were no failures for the fatigue test.

FBJ has been proven to be a viable method for joining advanced high-strength steels and aluminum. The FBJ method can exceed all of the minimum testing requirements that our automotive sponsor put forth. It also absorbs more energy on the cross-tension and t-peel tests than adhesives.

## 5.2 Recommendations

Further investigation is necessary to assess the ease of automating the process. Current research has used position control for the welding process, but load control should be studied to determine if there can be an improvement in the speed of the process. With the position control a "touch off" was required before the weld to establish the position of the bit.

# REFERENCES


Abe, Y., T. Kato and K. Mori (2009). "Self-piercing riveting of high tensile strength steel and aluminium alloy sheets using conventional rivet and die." Journal of materials processing technology **209**(8): 3914-3922.

Albrecht, S., M. Baumann, C. Brandstetter, R. Horn, H. Krieg, M. Fischer and R. Ilg (2013). "Environmental aspects of lightweight construction in mobility and manufacturing." Green Design, Materials and Manufacturing Processes: 185.

Barnes, T. A. and I. R. Pashby (2000). "Joining techniques for aluminium spaceframes used in automobiles: Part II — adhesive bonding and mechanical fasteners." Journal of Materials Processing Technology **99**(1–3): 72-79.

Bhagavathi, L. R., G. Chaudhari and S. Nath (2011). "Mechanical and corrosion behavior of plain low carbon dual-phase steels." Materials & Design **32**(1): 433-440.

Chen, C. and R. Kovacevic (2004). "Joining of Al 6061 alloy to AISI 1018 steel by combined effects of fusion and solid state welding." International Journal of Machine Tools and Manufacture **44**(11): 1205-1214.

Gendo, T., K. Nishiguchi, M. Asakawa and S. Tanioka (2007). Spot friction welding of aluminum to steel, SAE Technical Paper.

Hamel, V., J. M. Roelandt, J. N. Gacel and F. Schmit (2000). "Finite element modeling of clinch forming with automatic remeshing." Computers & Structures **77**(2): 185-200.

Huang, T., Y. Sato, H. Kokawa, M. Miles, K. Kohkonen, B. Siemssen, R. Steel and S. Packer (2009). "Microstructural evolution of DP980 steel during friction bit joining." Metallurgical and Materials Transactions A **40**(12): 2994-3000.

Kuziak, R., R. Kawalla and S. Waengler (2008). "Advanced high strength steels for automotive industry." Archives of civil and mechanical engineering **8**(2): 103-117.

Lim, Y. C., L. Squires, T.-Y. Pan, M. Miles, G.-L. Song, Y. Wang and Z. Feng (2015). "Study of mechanical joint strength of aluminum alloy 7075-T6 and dual phase steel 980 welded by friction bit joining and weld-bonding under corrosion medium." Materials & Design **69**: 37-43.

Marya, M. and X. Gayden (2005). "Development of requirements for resistance spot welding dual-phase (DP600) steels part 1—the causes of interfacial fracture." Welding Journal **84**(11): 172-182.

Matlock, D. K. and J. G. Speer (2009). Third generation of AHSS: microstructure design concepts. Microstructure and texture in steels, Springer**:** 185-205.

Miles, M., Z. Feng, K. Kohkonen, B. Weickum, R. Steel and L. Lev (2010). "Spot joining of AA 5754 and high strength steel sheets by consumable bit." Science and Technology of Welding & Joining **15**(4): 325-330.

Miles, M., S.-T. Hong, C. Woodward and Y.-H. Jeong (2013). "Spot welding of aluminum and cast iron by friction bit joining." International journal of precision engineering and manufacturing **14**(6): 1003-1006.

Miles, M., U. Karki and Y. Hovanski (2014). "Temperature and Material Flow Prediction in Friction-Stir Spot Welding of Advanced High-Strength Steel." JOM **66**(10): 2130-2136.

Miles, M., K. Kohkonen, S. Packer, R. Steel, B. Siemssen and Y. Sato (2009). "Solid state spot joining of sheet materials using consumable bit." Science and Technology of Welding and Joining **14**(1): 72-77.

Mori, K., T. Kato, Y. Abe and Y. Ravshanbek (2006). "Plastic Joining of Ultra High Strength Steel and Aluminium Alloy Sheets by Self Piercing Rivet." CIRP Annals - Manufacturing Technology **55**(1): 283-286.

Nandan, R., T. DebRoy and H. Bhadeshia (2008). "Recent advances in friction-stir welding–process, weldment structure and properties." Progress in Materials Science **53**(6): 980-1023.

Pan, T., A. Joaquin, D. E. Wilkosz, L. Reatherford, J. M. Nicholson, Z. Feng and M. L. Santella (2004). Spot friction welding for sheet aluminum joining. Proceedings of the 5th international symposium of friction stir welding, Metz, France.

Ram, T. (2015). "An Overview of High-Performance Aircraft Structural Al Alloy-AA7085." 金属学报: 英文版(7): 909-921.

Squires, L. P. (2014). "Friction Bit Joining of Dissimilar Combinations of Advanced High-Strength Steel and Aluminum Alloys."

Sun, Z. and R. Karppi (1996). "The application of electron beam welding for the joining of dissimilar metals: an overview." Journal of Materials Processing Technology **59**(3): 257-267.

Torkamany, M., S. Tahamtan and J. Sabbaghzadeh (2010). "Dissimilar welding of carbon steel to 5754 aluminum alloy by Nd: YAG pulsed laser." Materials & Design **31**(1): 458-465.

Yilbaş, B. S., A. Z. Şahin, N. Kahraman and A. Z. Al-Garni (1995). "Friction welding of St Al and Al Cu materials." Journal of Materials Processing Technology **49**(3–4): 431-443.

Zakaria, K. A., S. Abdullah and M. J. Ghazali (2013). "Comparative study of fatigue life behaviour of AA6061 and AA7075 alloys under spectrum loadings." Materials & Design **49**: 48-57.

APPENDIX A

The equation used to calculate the total work to failure for each sample is shown below. The numbers for each sample the numbers for the calculations came from tables similar to the table below. For the larger work load samples there were several thousand intervals.

$$\sum_{i}^{n} \boldsymbol{work_{i-1}} + \left(\frac{\boldsymbol{elongation_i - elongation_{i-1}}}{\mathbf{1000}}\right) \div \left(\frac{(\boldsymbol{load_i + load_{i-1}})}{\mathbf{2}}\right)$$

(Note: the elongation is converted to meters). An example for interval 2 in the table below (Compare with Table 12 Page 53) is shown in this equation.

$$\mathbf{0.004} + \left(\frac{\left(\frac{\mathbf{0.031 - 0.014}}{\mathbf{1000}}\right)}{\left(\frac{\mathbf{311.642 + 256.707}}{\mathbf{2}}\right)}\right) = \mathbf{0.008}$$